Chapter 12

OPTICAL PROPERTIES OF DIELECTRIC AND SEMICONDUCTOR THIN FILMS

I. Chambouleyron

Instituto de Física Gleb Wataghin, Universidade Estadual de Campinas—UNICAMP, 13083-970 Campinas, SP, Brazil

J. M. Martínez

Instituto de Matemática, Universidade Estadual de Campinas—UNICAMP, 13083-970 Campinas, SP, Brazil

Contents

1. THEORY

1.1. Historical Note

Interference phenomena of light waves occur frequently in nature, as in the colored reflection produced by feathers and wings of birds and many insects. The interference pattern given by oily substances onto water has been certainly noticed by man since ancient times. The origin of such effects, however, remained unclear until relatively recent times. The first systematic study on interference was undertaken by Newton [1], the well-known Newton rings, obtained from multiple reflections of light in the tiny air layer left between a flat and a little convex piece of glass. The effect, however, was not properly understood at that moment due to Newton's belief that light beams were the propagation of a stream of particles, Newton rejecting the idea of light being a wavelike perturbation of the ether. In 1690, Huygens [2] published his *Treatise on Light*, in which he proposed that light was a disturbance propagating through the ether as sound moves through air. There is no reference to wavelengths, though, or a connection of these and color. In 1768, Euler [3] advanced the hypothesis that the colors we see depends on the wavelength of wave light, in the same way as the pitch of the sound we hear depends on the wavelength of sound. In 1801, in the lecture *On the theory of light and colors*, delivered before the Royal Society, Young sketched the current theory of color vision in terms of three different (pri-

Handbook of Thin Films Materials, edited by H.S. Nalwa
Volume 3: Volume Title

mary) colors. Young's experiments on the interference of two light beams [4] were made around 1800 and published in 1807. They gave the ultimate proof of the wave nature of light and allowed the determination of the wavelength of visible light. In the words of Herschel [5], "... Dr. Young has established a principle in optics, which, regarded as a physical law, has hardly its equal for beauty, simplicity, and extent of applications, in the whole circle of science.... The experimental means by which Dr. Young confirmed this principle, which is known in optics by the name of interference of the rays of light, were as simple and satisfactory as the principle itself is beautiful. ... Newton's colors of thin films were the first phenomena to which the author applied it with full success." Based on the experiments of Malus on the polarization of light by ordinary reflection at the surface of a transparent body, Young proposed a few years later that light waves were transverse perturbations of the ether and not longitudinal, as sound waves. The consequences of the finding kept physicists busy for the next hundred years. It was Fresnel that put Young's results on a firm mathematical basis. He established the relations between the amplitudes of the reflected and refracted waves and the incident waves, known as the Fresnel formulae.

Optical coatings remained a subject of laboratory curiosity in the sense that no industrial applications occurred until the twentieth century, with the notable exception of mirror production. Until the late Middle Ages, mirrors were simply polished metals. At a certain unknown moment, the Venetian glass workers introduced glass silvering using an amalgam of tin and mercury [6]. The method lasted until the nineteenth century, when the backing of glass was made with silver. The development of vacuum apparatus techniques allowed the evaporation of a large class of materials, with the ensuing application to optical systems, among others. The methods to deposit thin films in a controllable way increased at a rapid pace, as did the applications to different fields of industry. Today, advanced electronic and optical devices are manufactured involving single or multilayered structures of materials of very different nature: electro-optic and optical materials, semiconductors, insulators, superconductors, and all kinds of oxide and nitride alloys. This rapid development demands accurate deposition methods, sometimes with *in situ* characterization, as well as powerful algorithms for fast corrections to predicted performance.

1.2. The General Problem

Figure 1 sketches the general problem. A beam of mono- or polychromatic light falls onto a p-layered optical structure. Within the structure, or at the interfaces, light may be absorbed and/or scattered. In general, the thickness of the different optical coatings composing the structure varies between 0.05 and a few times the wavelength of the incident light beam. An abrupt interface between materials of different optical properties (or a discontinuity taking place in a distance small compared with the light wavelength) provokes a partial reflection of the light beam. Sometimes, a change of phase also occurs. As the distances between layer boundaries are comparable to the photon wavelength, multiplyreflected or transmitted beams are coherent with one another. Consequently, the total amount of light reflected and transmitted by the structure results from the algebraic sum of the amplitudes of these partially reflected and partially transmitted beams. This property is at the base of a large number of applications. Depending on the specific case, the substrate (S) supporting the structure may be transparent or absorbing. Self-supported structures may be built also but, in what follows, the existence of a thick supporting substrate will be assumed. Hence, in the present context, a thin film is equivalent to an optical coating.

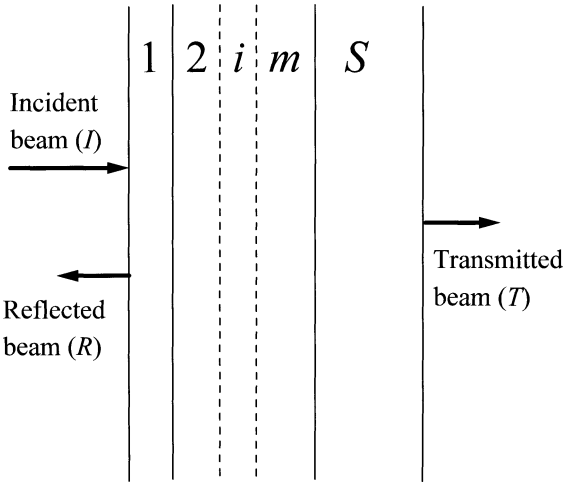

Fig. 1. The figure sketches the general optical coating problem. A light beam impinges onto a stack of dielectric thin layers supported by thick substrate. The radiation is partly transmitted and partly reflected, both depending on photon energy and layer thickness. Part of the radiation may be internally absorbed.

The structure depicted in Figure 1 suggests three different problems:

(a) *Optical response*. Calculation of the spectral response of a p-layered structure deposited onto a substrate of known properties. The optical constants of the coating materials as a function of photon wavelength are given, as well as the thickness of each layer.
(b) *Structure design*. The problem here is to find the appropriate materials, the number of layers, and their respective thicknesses in order to meet a desired spectral performance.
(c) *Reverse optical engineering*. Retrieval of the optical parameters and the thicknesses of the layers composing the structure from measured spectral responses.

In mathematical terms, the *optical response* problem is a *direct* problem. The phenomenon is governed by a partial differential wave equation (coming from Maxwell equations) where we assume that the parameters and boundary conditions are given. The direct problem consists of computing the state of the wave within each layer, using the information mentioned above.

Analytic solutions can be given if we assume that the incident wave is a *pure* wave and that the boundary layers are regular. In more complicated situations, numerical solutions are necessary. However, even in the case where analytic calculations are possible, the practical computation of the response can be very costly. This is because pure waves do not exist in most optical experiments, and the true response corresponds to an average among many waves of different wavelength. Although it is possible to give the transmitted and reflected energies of pure waves in a closed analytic form, their analytic integration cannot be done and the numerical integration process is, computationally, very expensive.

Design and *reverse engineering* problems are inverse problems in the sense that, in both cases, the response of the system (or a part of it, such as transmitted or reflected energy for a set of wavelengths) is known, but (some of) the parameters producing this response must be estimated. In *design* problems, we have a "target response" but there is no *a priori* knowledge of whether or not it is possible to obtain that response for some set of boundary conditions. In *reverse optical* problems, the response of the structure has already been measured but the specific conditions under which it has been generated are not known. The key tool for an efficient solution of *design* and *reverse engineering* problems is an adequate code that solves the optical response problem. All computational devices used to solve those problems obey the following general scheme: (i) try a set of parameters; (ii) solve the optical response problems using them; (iii) accept the parameters if the response is satisfactory and change them in a suitable way if it is not. This is also the scheme of most optimization algorithms, which try to minimize (or maximize) some objective function subject to a set of constraints. The choice of the objective (or merit) function to be used depends on the nature of the problem. Smoothness considerations usually lead to the use of some kind of sum of squares of experimental data.

Some features complicating the optimization of *design* and *reverse engineering* problems are:

(1) *Local nonglobal minimizers*. In some problems, the solution is well defined but, out of this solution, the merit function presents a highly oscillatory behavior with similar functional values. In other words, the function has many local (nonglobal) minimizers which are useless for design or estimation purposes. Most efficient optimization algorithms have guaranteed convergence to local minimizers (in fact, something less than that) but not to global minimizers, so they tend to get stuck in the attraction basin of those undesirable local minimizers.

(2) *Ill-posedness*. Some mathematical problems can be highly underdetermined, the solution not being unique. Adding to this feature the fact that additional errors due to small inadequacies of the model can be present, we have situations where an infinite set of mathematical approximate solutions can be found, but where the *true physical solution* may not correspond to the point with smallest merit function value. This feature is typical in the so-called *inverse problems* in the estimation literature. The ill-posedness problem can be partially surmounted by introducing, in the model, some prior information on the behavior of the parameters to be estimated. When our knowledge of this behavior is poor, we can use regularization processes [7]. Finally, instead of the *true* expensive models, simplified direct algorithms can be used which, sometimes, are sufficient to find suitable estimates of the parameters, or a good enough approximation to them.

(3) *Expensive models*. Problems (1) and (2) become more serious if the solution of the associated direct problem is computationally expensive. Optimization algorithms need, essentially, trial-and-error evaluations of the optical response and, obviously, if this evaluation demands a great deal of computer time, the possibility of obtaining good practical solutions in a reasonable period of time is severely diminished. Partial solutions to all the difficulties mentioned above have been found. The multiple-local-minimizers problem can be attacked by the use of *global optimization algorithms* that, in principle, are able to jump over undesirable local nonglobal solutions. However, all these procedures are computationally expensive, and their effectiveness is linked to the possibility of overcoming this limitation.

For the sake of completeness, let us note that all these remedies may fail. No global optimization method guarantees the finding of global minimizers of any function in a reasonable time. The information that must be introduced into the problem to enhance the probability of finding a good estimate of the parameters is not always evident. Moreover, it is not always clear in which way the information must be introduced in the model. Finally, it is not known how much an optical response problem can be simplified without destroying its essential characteristics. As in many inverse problems exhaustively analyzed in the literature, each particular situation must be studied from scratch (although, of course, experience in similar situations is quite useful) and can demand original solutions. In this review, we consider the reverse solution of some simple optical structures.

The structure shown in Figure 1 calls for some additional considerations.

(1) In principle, the angle of incidence of the impinging beam may be any angle, the simplest case being that of normal incidence. The mathematical formulation of the problem for light arriving at angles other than normal to the surface of the coatings becomes more involved. The general case is treated in a coming section.

(2) The coatings and the substrate are optically homogeneous and isotropic. The surfaces and the interfaces between layers are perfectly flat and parallel to each other. In other words, we will not consider the case of rough surfaces producing some scattering of the light, nor the existence of thickness gradients or inhomogeneities. The effects produced by these deviations to the ideal case will not be discussed. See [8, 9].

(3) In this chapter, we review the properties and applications of semiconductor and dielectric thin films; that is, metal coatings are not included.

1.3. Light–Matter Interaction

Dielectric and semiconductor coatings are films of materials having strong ionic or directed covalent bonds. In most cases, they are transparent to visible and/or infrared light. The interaction of the electromagnetic radiation with these films is treated by applying boundary conditions to the solutions of Maxwell equations at the boundary between different media. In the field of optical coatings, the wavelength of the light is always very much larger than interatomic dimensions. Thus the interaction of light and matter is averaged over many unit cells. As a consequence, the optical properties within each layer can be described macroscopically in terms of phenomenological parameters, the so-called optical constants or optical parameters. As shown below, these are the real and the imaginary parts of a complex index of refraction $\widetilde{n}$. The real part, $n(\lambda)$, is the ratio of the velocity of light in vacuum to the velocity of light of wavelength (λ) in the material. The imaginary part, $-\kappa(\lambda)$, is an attenuation coefficient measuring the absorption of light with distance. Using Maxwell equations, it is possible to relate these frequency-dependent "constants" to other optical parameters such as the dielectric constant and the conductivity.

The coating materials are composed of charged particles: bound and conduction electrons, ionic cores, impurities, etc. These particles move differently with oscillating electric fields, giving rise to polarization effects. At visible and infrared light frequencies, the only contribution to polarization comes from the displacement of the electron cloud, which produces an induced dipole moment. At frequencies smaller than these, other contributions may appear, but they are of no interest to the purpose of the present work. The parameters describing these optical effects, that is, the dielectric constant ε, the dielectric susceptibility χ, and the conductivity σ, can be treated as scalars for isotropic materials. In what follows, dielectric and semiconductor coating materials are considered nonmagnetic and have no extra charges other than those bound in atoms.

To find out what kind of electromagnetic waves exist inside dielectric films, we take $\rho = -\nabla \cdot \mathbf{P}$ and $\mathbf{j} = \partial \mathbf{P}/\partial t$, where ρ is an effective charge, $\mathbf{P}$ is the polarization induced by the electromagnetic wave, assumed to be proportional to the electric field, and $\mathbf{j}$ is the corresponding current density averaged over a small volume. Under these conditions, average field Maxwell equations in MKS units read:

$$\begin{aligned} \nabla \cdot \mathbf{E} &= -\frac{\nabla \cdot \mathbf{P}}{\varepsilon_0} \\ \nabla \times \mathbf{E} &= -\frac{\partial \mathbf{B}}{\partial t} \\ \nabla \cdot \mathbf{B} &= 0 \\ c^2 \nabla \times \mathbf{B} &= \frac{\partial}{\partial t}\left(\frac{\mathbf{P}}{\varepsilon_0} + \mathbf{E}\right) \end{aligned}$$

where the symbols have their usual meaning. Note that the normal component of the electric field $\mathbf{E}$ is not conserved at the interface between materials of different polarizability. Instead, $\mathbf{D} = \varepsilon_0 + \mathbf{P}$, called electrical displacement, is conserved across such interfaces. The solutions to these equations have the form of harmonic plane waves with wave vector k:

$$\begin{aligned} \mathbf{E} &= \mathbf{E}_0 \exp\left[i(\omega t - k \cdot r)\right] \\ \mathbf{H} &= \mathbf{H}_0 \exp\left[i(\omega t - k \cdot r)\right] \end{aligned}$$

and represent a wave traveling with a phase velocity $\omega/k = c/n$, where c is the speed of light in vacuum and n is the index of refraction. When optical absorption is present, the wave vector and the index are complex quantities. From the Maxwell equations, a dispersion relation $k^2 = \varepsilon(\omega/c)^2$ is obtained relating the time variation with the spatial variation of the perturbation.

In general, then, the wave vector k and the dielectric constant ε are complex quantities, that is, $\widetilde{k} = k_1 - ik_2$ and $\widetilde{\varepsilon} = \varepsilon_1 - i\varepsilon_2$. It is useful to define a complex index of refraction:

$$\widetilde{n} \equiv \widetilde{k}\left(\frac{c}{\omega}\right) = n - i\kappa$$

For isotropic materials, k_1 and k_2 are parallel and

$$\varepsilon_1 = n^2 - \kappa^2 \qquad \varepsilon_2 = 2n\kappa$$

with the converse equations,

$$n^2 = \frac{1}{2}\left[\varepsilon_1 + \left(\varepsilon_1^2 + \varepsilon_2^2\right)^{1/2}\right] \qquad \kappa^2 = \frac{1}{2}\left[-\varepsilon_1 + \left(\varepsilon_1^2 + \varepsilon_2^2\right)^{1/2}\right]$$

In the photon energy region where ε is real, $n = \varepsilon^{1/2}$ is also real and the phase (ω/k) and group $(\partial\omega/\partial k)$ velocities are equal to c/n. In general, the velocity is reduced to $v(\lambda) = 1/\sqrt{\varepsilon_c(\lambda)}$ in a medium of a complex dielectric constant ε_c. The real part of n determines the phase velocity of the light wave, the imaginary part determining the spatial decay of its amplitude. The absorption coefficient α measures the intensity loss of the wave. For a beam traveling in the z direction, $I(x) = I(0)\exp(-\alpha z)$, which means $\alpha = 2\omega\kappa/c = 4k\kappa/\lambda$. See [8].

Optical Properties of Dielectric Films

The main absorption process in semiconductors and dielectrics originates from the interaction of light with electrons [10–12]. If the photon has a frequency such that its energy matches the energy needed to excite an electron to a higher allowed state, then the photon may be absorbed. The electron may be an ion-core electron or a free electron in the solid. If the energy of the incoming photon does not match the required excitation energy, no excitation occurs and the material is transparent to such radiation. In nonmetal solids, there is a minimum energy separating the highest filled electron states (valence band) and the lowest empty ones (conduction band), known as the energy band-gap. Electron transitions from band to band constitute the strongest source of absorption. In dielectrics, such as glass, quartz, some salts, diamond, many metal oxides, and most plastic materials, no excitation resonances exist in the visible spectrum, because the valence electrons are so tightly bound that photons with energy in the ultraviolet are necessary to free them. Ideally, photons having an energy smaller than the band-gap are not absorbed. On the contrary, metals are

good reflectors and are opaque to visible and infrared radiation. Both effects derive from the existence of a large density of free electrons which are able to move so freely that no electric field may propagate within the solid. The reflecting properties of metals find numerous optical applications, as in mirrors.

The optical properties of semiconductors lie between those of metals and those of insulating dielectrics. Semiconductors are normally transparent in the near infrared and absorbing in the visible spectrum, whereas the absorption in dielectrics is strong in the ultraviolet. Thus, the fundamental absorption edge of semiconductors lies, approximately, between 0.5 eV ($\lambda \sim$ 2500 nm) and 2.5 eV ($\lambda \sim$ 500 nm). Within a small energy range around the fundamental absorption edge, semiconductors go, ideally, from high transparency to complete opacity. However, the presence of impurities, free conduction electrons or holes, and/or other defect states may affect the transparency of semiconductor and dielectric materials at photon energies smaller than the band-gap.

The situation just depicted is ideal in the sense that we have considered *perfect* dielectric and semiconductor crystalline materials. In most cases, however, the deposited optical coatings are either microcrystalline or amorphous. Microcrystalline layers are formed by the aggregation of randomly oriented small crystals having a typical size of the order of the film thickness. The regions between crystallites, or grain boundaries, are highly imperfect regions having a large density of localized electron states located at energies between the valence and conduction bands. These surface or interface defect states constitute a source of absorption; that is, electrons are excited from the valence band to localized states and/or from them to the conduction band. In all cases, however, the absorption due to defects is smaller than that of the fundamental edge, but it may affect in a nonnegligible way the optical properties of the coating.

The fundamental characteristic of an amorphous material is the topological disorder. The atoms of an amorphous network do not form a perfect periodic array as in crystalline materials. The absence of periodicity, or of long-range order, has important consequences on the optical properties of the films. Disorder induces the appearance of localized electron states within the band-gap. These localized states are of two types: coordination defects, also called dangling bonds or deep defects, and valence and conduction band tail states (shallow states). Both contribute to the absorption of light. Most important, due to the lack of periodicity, the electron wave vector $\vec{k}$ is no longer a good quantum number and the selection rules, valid for optical transitions in crystals, break down. As a consequence, more transitions are allowed between electron states with an energy separation equal to the photon energy. The absorption coefficient due to-band-to band transitions is much larger in amorphous dielectrics and semiconductors than in their crystalline parents. The density of defect states and the corresponding optical absorption strength depend strongly on deposition methods and conditions.

The Absorption Edge of Semiconductors and Dielectrics

In general, the process of electron excitation by photon absorption is very selective. The sharpness of absorption lines is clearly noted in the dark lines of atomic spectra. The requirement of energy matching, called resonance, must also be met in solids, but solids have such an abundant range of possible excitations that absorption occurs in a broad energy range. Even so, many of the optical properties of materials around resonances can be understood in terms of the properties of a damped harmonic oscillator, often called the Lorentz oscillator. In the model, it is assumed that the electrons are bound to their cores by harmonic forces. In the presence of an external field $E_0 \exp(-i\omega t)$, their motion is given by

$$m\frac{\partial^2 r}{\partial t^2} + m\gamma\frac{\partial r}{\partial t} + m\omega_0^2 r = -eE\exp(-i\omega t)$$

where m and e are the mass and the charge of the electron, ω_0 is the natural frequency of the oscillator, and γ is a damping term. Solving for the electron displacement $r = r_0 \exp(-i\omega t)$, one gets

$$r = \frac{-eE/m}{(\omega_0^2 - \omega^2) - i\gamma\omega}$$

The response of a system having a density N/V of such oscillators can be obtained in terms of the induced polarization:

$$P = -erN/V = \frac{(e^2 N/mV)E}{(\omega_0^2 - \omega^2) - i\gamma\omega}$$

The dielectric constant corresponding to this polarization is

$$\tilde{\varepsilon} = \varepsilon_1 - i\varepsilon_2 = 1 - \text{const} \cdot \frac{1}{(\omega_0^2 - \omega^2 - i\gamma\omega)}$$

with

$$\varepsilon_1 = n_r^2 - \kappa^2 = 1 - K\frac{(\omega_0^2 - \omega^2)}{(\omega_0^2 - \omega^2)^2 + \gamma^2\omega^2}$$

$$\varepsilon_2 = 2n_r\kappa = K\frac{\gamma\omega}{(\omega_0^2 - \omega^2)^2 + \gamma^2\omega^2}$$

where K is a constant. Figure 2 shows the shape of the real and imaginary parts of the dielectric constant of a Lorentz oscillator. This model is extremely powerful because, in real systems, it describes quite accurately not only the absorption between bands, but also that corresponding to free electrons and phonon systems. The reason for the general applicability of the Lorentz oscillator is that the corresponding quantum-mechanical equation for ε, not discussed here, has the same form as the classical equation for the damped oscillator.

In a solid dielectric, resonances at different frequencies having different loss values contribute to the dielectric response with terms having a shape similar to that shown in Figure 2. The overall dielectric response results from the addition of all these contributions, as shown in Figure 3 for a hypothetical semiconductor. For photon energies smaller than the band-gap ($\hbar\omega < E_G$), the material is transparent or partially absorbing. This is the *normal dispersion* frequency range in which both

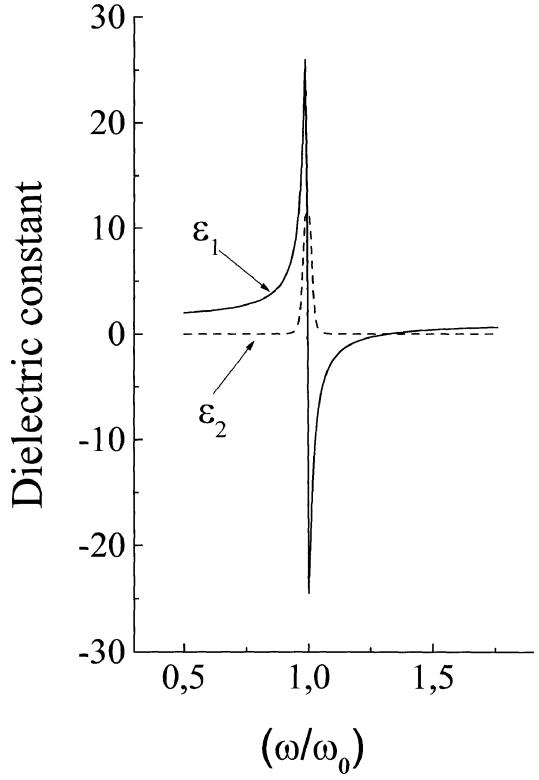

Fig. 2. Characteristic behavior of the real and the imaginary part of the dielectric constant of a classical damped electron oscillator as a function of the relative excitation frequency (Lorentz oscillator).

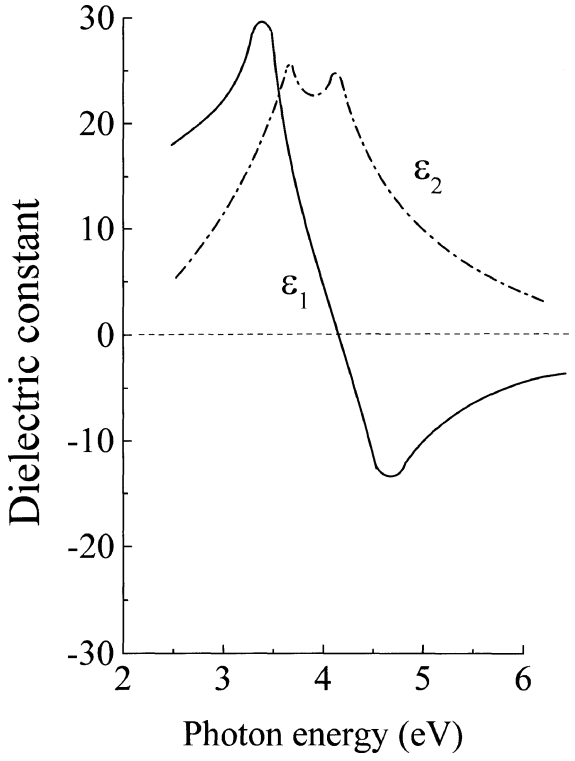

Fig. 3. Real and imaginary parts of a hypothetical semiconductor as a function of photon energy.

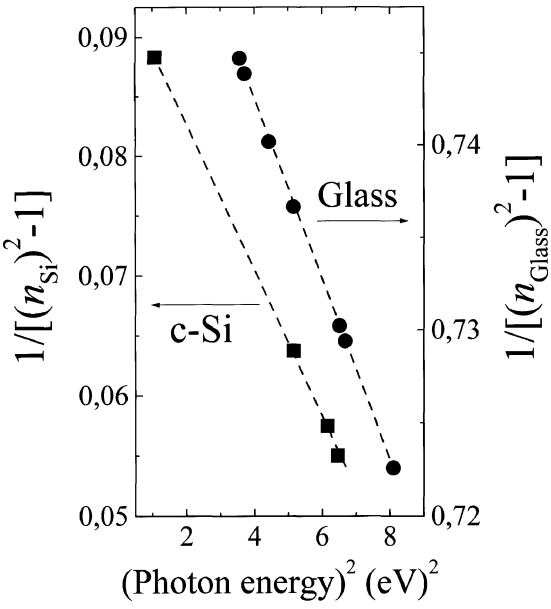

Fig. 4. Single-effective-oscillator representation of the index of refraction of crystalline silicon and of an optical glass as a function of the square of photon energy.

the index of refraction and the absorption increase with photon energy. Moreover, the slope of $\partial n/\partial(\hbar\omega)$ also increases with increasing photon energy. It is important to remark at this point that the refractive index dispersion data below the interband absorption edge of a large quantity of solids can be plotted using a single-effective-oscillator fit of the form $n^2 - 1 = F_d F_0/(F_0^2 - \hbar^2\omega^2)$, where F_0 is the single-oscillator energy, and F_d is the dispersion energy [13]. These parameters obey simple empirical rules in large groups of covalent and ionic materials. Figure 4 shows the single-effective-oscillator representation of the refractive index of an optical glass and of crystalline silicon. The fit is very good for a wide photon energy range.

Let us end the section with a few words on the shape of the absorption edge in crystalline and amorphous layers. The absorption coefficient has an energy dependence near the absorption edge expressed as $\alpha \approx (\hbar\omega - E_G)^s$, where s is a constant. In the one-electron approximation, the values taken by s depend on the selection rules for optical transitions and on the material's band structure. For allowed transitions, $s = 1/2$ for direct transitions (i.e., GaAs) and $s = 2$ for indirect transitions (i.e., Si or Ge). In amorphous materials, the absorption edge always displays an exponential dependence on photon energy. The characteristic energy of the exponential edge, called Urbach energy, depends on the material and on deposition conditions [14, 15].

For reasons that will become clear in a forthcoming section, knowledge of the physics behind the dependence of the optical constants on photon energy may be of great help in solving optical reverse engineering problems.

1.4. Basic Formulae for Transmitted and Reflected Waves

1.4.1. Single Interface

Consider the complex wave function

$$\widetilde{u}_I(z,t) = \widetilde{E}_I \exp\left[i\left(\omega t - \widetilde{k}_0 z\right)\right] \tag{1}$$

where ω is real and nonnegative, whereas $\widetilde{E}_I$ and $\widetilde{k}_0$ are complex. By (1), the wavelength λ is $2\pi/|\Re(\widetilde{k}_0)|$. ($\Re(z)$ will denote always the real part of the complex number z and $\Im(z)$ denotes its imaginary part.) So,

$$\left|\Re\left(\widetilde{k}_0\right)\right| = \frac{2\pi}{\lambda} \tag{2}$$

Let the complex number

$$\widetilde{n}_0 = n_0 - i\kappa_0$$

denote the generalized index of refraction in the $x-$ domain of u, and

$$\widetilde{k}_0 = \pm\frac{\omega\widetilde{n}_0}{c} \tag{3}$$

If $\Re(k) > 0$, the wave travels in the forward direction, whereas if $\Re(k) < 0$, the wave goes backwards.

Assume now that (1) is an "incident" wave, defined for $z \le L$, arriving at an abrupt interface (xy plane) between two different media at $z = L$. As sketched in Figure 5, this wave generates a "transmitted" wave $\widetilde{u}_T$, defined for $z \ge L$, and a "reflected" wave $\widetilde{u}_R$, defined for $z \le L$. Let us write

$$\widetilde{u}_T(z,t) = \widetilde{E}_T \exp\left[i\left(\omega_T t - \widetilde{k}_T z\right)\right] \tag{4}$$

and

$$\widetilde{u}_R(z,t) = \widetilde{E}_R \exp\left[i\left(\omega_R t - \widetilde{k}_R z\right)\right] \tag{5}$$

Assume that the complex number $\widetilde{n}_1$ is the generalized index of refraction of the layer $z > L$.

Continuity in $z = L$ imposes:

$$\begin{aligned}&\widetilde{E}_I \exp\left[i\left(\omega t - \widetilde{k}_0 L\right)\right] + \widetilde{E}_R \exp\left[i\left(\omega_R t - \widetilde{k}_R L\right)\right]\\ &\quad = \widetilde{E}_T \exp\left[i\left(\omega_T t - \widetilde{k}_T L\right)\right]\end{aligned}$$

for all real t. So,

$$\begin{aligned}&\widetilde{E}_I \exp\left(-i\widetilde{k}_0 L\right)\exp[i\omega t] + \widetilde{E}_R \exp\left(-i\widetilde{k}_R L\right)\exp[i\omega_R t]\\ &\quad = \widetilde{E}_T \exp\left(-i\widetilde{k}_T L\right)\exp[i\omega_T t]\end{aligned}$$

for all $t \in \mathbb{R}$. Since this identity is valid for all t, we must have

$$\omega_R = \omega_T = \omega$$

Now, the direction of the reflected wave must be opposite to that of the incident wave, and the direction of the transmitted wave must be the same. So, by (3),

$$\widetilde{k}_R = -\widetilde{k}_0 \qquad \widetilde{k}_T = \frac{\widetilde{n}_1}{\widetilde{n}_0}\widetilde{k}_0$$

Therefore,

$$\widetilde{E}_I \exp\left(-i\widetilde{k}_0 L\right) + \widetilde{E}_R \exp\left(i\widetilde{k}_0 L\right) = \widetilde{E}_T \exp\left(-i\frac{\widetilde{n}_1}{\widetilde{n}}\widetilde{k}_0 L\right) \tag{6}$$

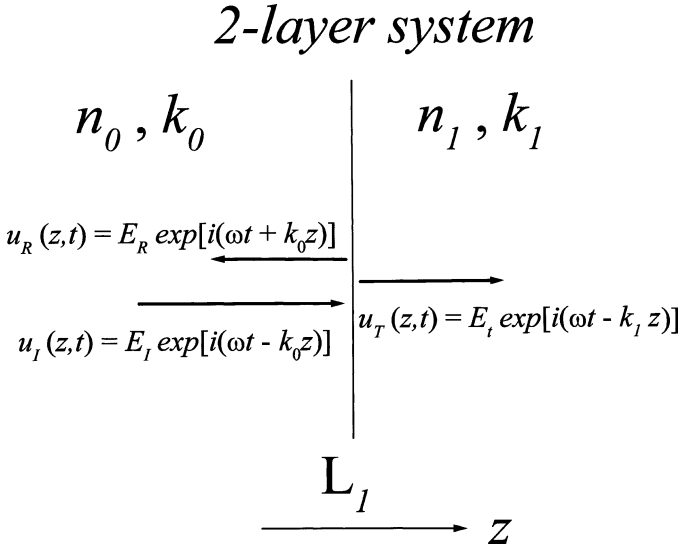

Fig. 5. Incident, reflected, and transmitted waves at an abrupt interface between two different media.

Now, using continuity of the derivative with respect to z in $z = L$, and the above expressions of $\omega_R, \omega_T, \widetilde{k}_R, \widetilde{k}_T$, we have

$$\begin{aligned}&\left(-i\widetilde{k}_0\right)\widetilde{E}_I \exp\left[i\left(\omega t - \widetilde{k}_0 z\right)\right] + \left(i\widetilde{k}_0\right)\widetilde{E}_R \exp\left[i\left(\omega t + \widetilde{k}_0 z\right)\right]\\ &\quad = -i\widetilde{k}\frac{\widetilde{n}_1}{\widetilde{n}_0}\widetilde{E}_T \exp\left[i\left(\omega t - \frac{\widetilde{n}_1}{\widetilde{n}_0}\widetilde{k}_0 z\right)\right]\end{aligned}$$

for $z = L$ and for all $t \in \mathbb{R}$. Therefore,

$$\begin{aligned}&\widetilde{E}_I \exp\left[i\left(\omega t - \widetilde{k}_0 L\right)\right] - \widetilde{E}_R \exp\left[i\left(\omega t + \widetilde{k}_0 L\right)\right]\\ &\quad = \frac{\widetilde{n}_1}{\widetilde{n}_0}\widetilde{E}_T \exp\left[i\left(\omega t - \frac{\widetilde{n}_1}{\widetilde{n}_0}\widetilde{k}_0 L\right)\right]\end{aligned}$$

Thus,

$$\begin{aligned}&\widetilde{E}_I \exp\left(-i\widetilde{k}_0 L\right)\exp[i\omega t] - \widetilde{E}_R \exp\left(i\widetilde{k}_0 L\right)\exp[i\omega t]\\ &\quad = \frac{\widetilde{n}_1}{\widetilde{n}_0}\widetilde{E}_T \exp\left[-i\frac{\widetilde{n}_1}{\widetilde{n}_0}\widetilde{k}_0 L\right]\exp[i\omega t]\end{aligned}$$

which implies

$$\widetilde{E}_I \exp\left(-i\widetilde{k}_0 L\right) - \widetilde{E}_R \exp\left(i\widetilde{k}_0 L\right) = \frac{\widetilde{n}_1}{\widetilde{n}_0}\widetilde{E}_T \exp\left[-i\frac{\widetilde{n}_1}{\widetilde{n}_0}\widetilde{k}_0 L\right] \tag{7}$$

Adding (6) and (7), we get

$$2\widetilde{E}_I \exp\left(-i\widetilde{k}_0 L\right) = \left[1 + \frac{\widetilde{n}_1}{\widetilde{n}_0}\right]\widetilde{E}_T \exp\left[-i\frac{\widetilde{n}_1}{\widetilde{n}_0}\widetilde{k}_0 L\right]$$

Therefore,

$$\left[1 + \frac{\widetilde{n}_1}{\widetilde{n}_0}\right]\widetilde{E}_T = 2\widetilde{E}_I \exp\left[-i\widetilde{k}_0 L\left(1 - \frac{\widetilde{n}_1}{\widetilde{n}_0}\right)\right]$$

so,

$$\widetilde{E}_T = \frac{2\widetilde{n}}{\widetilde{n} + \widetilde{n}_1}\widetilde{E}_I \exp\left[i\widetilde{k}_0 L\left(\frac{\widetilde{n}_1}{\widetilde{n}_0} - 1\right)\right] \tag{8}$$

Subtracting (7) from (6), we obtain

$$2\widetilde{E}_R \exp\bigl(i\widetilde{k}_0 L\bigr) = \left(1 - \frac{\widetilde{n}_1}{\widetilde{n}_0}\right)\widetilde{E}_T \exp\left[-i\frac{\widetilde{n}_1}{\widetilde{n}_0}\widetilde{k}_0 L\right] = \left(1 - \frac{\widetilde{n}_1}{\widetilde{n}_0}\right)\frac{2\widetilde{n}_0}{\widetilde{n}_0 + \widetilde{n}_1}\widetilde{E}_I \exp\bigl(-i\widetilde{k}_0 L\bigr)$$

So,

$$\widetilde{E}_R = \frac{\widetilde{n}_0 - \widetilde{n}_1}{\widetilde{n}_0 + \widetilde{n}_1}\widetilde{E}_I \exp\bigl(-2i\widetilde{k}_0 L\bigr) \tag{9}$$

Summing up:

If the incident wave acting on $z < L$ is

$$\widetilde{u}_I(z,t) = \widetilde{E}_I \exp\bigl[i\bigl(\omega t - \widetilde{k}_0 z\bigr)\bigr]$$

then the reflected wave ($z < L$) is

$$\widetilde{u}_R(z,t) = \frac{\widetilde{n}_0 - \widetilde{n}_1}{\widetilde{n}_0 + \widetilde{n}_1}\widetilde{E}_I \exp\bigl(-2i\widetilde{k}_0 L\bigr)\exp\bigl[i\bigl(\omega t + \widetilde{k}_0 z\bigr)\bigr] \tag{10}$$

and the transmitted wave ($z > L$) is

$$\widetilde{u}_T(z,t) = \frac{2\widetilde{n}_0}{\widetilde{n}_0 + \widetilde{n}_1}\widetilde{E}_I \exp\left[i\widetilde{k}_0 L\left(\frac{\widetilde{n}_1}{\widetilde{n}_0} - 1\right)\right] \times \exp\left[i\left(\omega t - \frac{\widetilde{n}_1}{\widetilde{n}_0}\widetilde{k}_0 z\right)\right] \tag{11}$$

1.4.2. Recursive Formulae for m Layers

Assume now, as shown in Figure 6, a system of m layers with generalized index of refraction $\widetilde{n}_0, \widetilde{n}_1, \ldots, \widetilde{n}_{m-1}$, respectively, separated by abrupt interfaces at $z = L_1$, $z = L_2, \ldots$, $z = L_{m-1}$, where $L_1 < L_2 < \cdots < L_{m-1}$. We identify each layer with its refractive index. The incident wave (defined for $z < L_1$) in the layer $\widetilde{n}_0$ is given by (1). The incident wave generates multiple reflected and transmitted waves in all the layers, as sketched in Figure 7. It is easy to verify that the ω-coefficient of all these generated waves is ω. Moreover, in the layer $\widetilde{n}_{m-1}$ ($z > L_{m-1}$), the k-coefficient of the transmitted wave will be $\widetilde{k}_0\widetilde{n}_{m-1}/\widetilde{n}_0$. The incident wave will also generate a reflected wave in $z < L_1$ whose k-coefficient will be $-\widetilde{k}_0$.

Mutatis mutandi, if the incident wave is defined in $z > L_{m-1}$ and given by $E_I \exp[i(\omega t + \widetilde{k}_{m-1} z)]$, the transmitted wave in $z < L_1$ has a k-coefficient equal to $\widetilde{k}_{m-1}\widetilde{n}_0/\widetilde{n}_{m-1}$ and the reflected wave in $z > L_{m-1}$ will have $-\widetilde{k}_{m-1}$ as k-coefficient. The ω-coefficient is always the same.

In this section, we deduce how the E-coefficient of the transmitted and reflected waves depends on the parameters of the incident wave. We define the coefficients $t_{0,m-1}$, $r_{0,m-1}$, $t_{m-1,0}$, $r_{m-1,0}$ in the following way:

(a) $t_{0,m-1}\widetilde{E}$ is the E-coefficient of the transmitted wave in the $\widetilde{n}_{m-1}$ layer generated by the wave (1) in layer $\widetilde{n}_0$.

(b) $r_{0,m-1}\widetilde{E}$ is the E-coefficient of the reflected wave in the $\widetilde{n}_0$ layer generated by the wave (1) in layer $\widetilde{n}_0$.

(c) $t_{m-1,0}\widetilde{E}$ is the E-coefficient of the transmitted wave in the layer $\widetilde{n}_0$, generated by a wave (1) defined in layer $\widetilde{n}_{m-1}$.

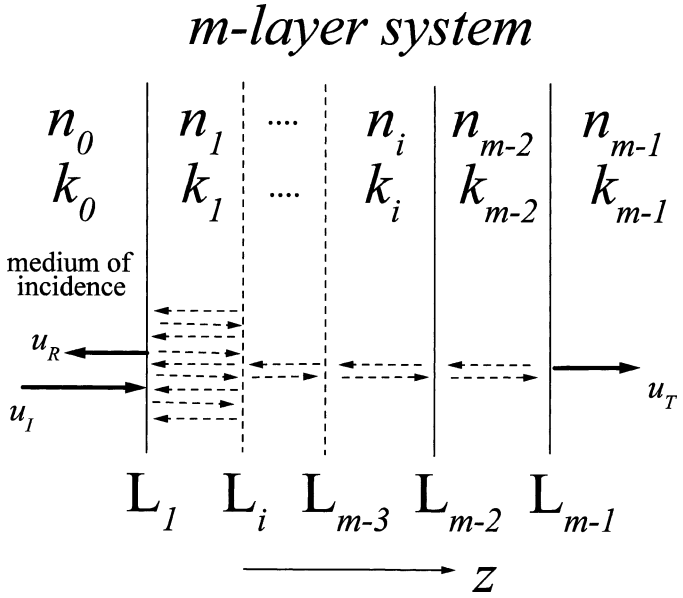

Fig. 6. Structure of an m-layered optical film system. The figure illustrates multiple reflections inside each layer characterized by a refractive index and an extinction coefficient.

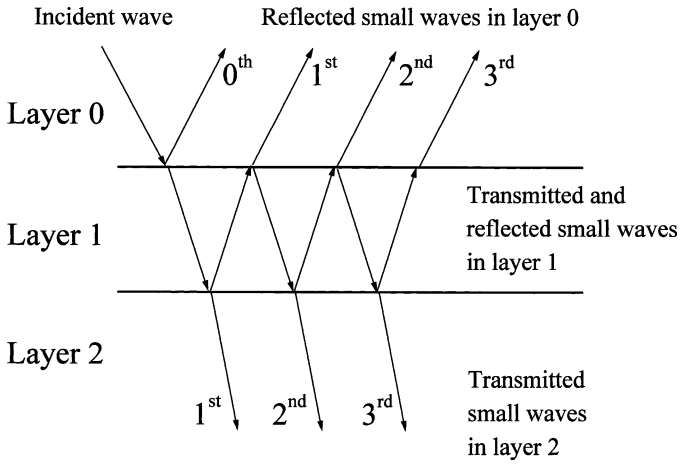

Fig. 7. Sketch of the multiple transmitted and reflected waves in a multilayer system.

(d) $r_{m-1,0}\widetilde{E}$ is the E-coefficient of the reflected wave in the $\widetilde{n}_{m-1}$ layer generated by a wave (1) defined in layer $\widetilde{n}_{m-1}$.

For completeness, we will write, when necessary:

$$t_{0,m-1} = t_{0,m-1}(\widetilde{k}) = t_{0,m-1}\bigl(\widetilde{k}_0, \widetilde{n}_0, \widetilde{n}_1, \ldots, \widetilde{n}_{m-1}, L_1, L_2, \ldots, L_{m-1}\bigr)$$

$$r_{0,m-1} = r_{0,m-1}(\widetilde{k}) = r_{1,m}\bigl(\widetilde{k}_0, \widetilde{n}_0, \widetilde{n}_1, \ldots, \widetilde{n}_{m-1}, L_1, L_2, \ldots, L_{m-1}\bigr)$$

$$t_{m-1,0} = t_{m-1,0}(\widetilde{k}) = t_{m,1}\bigl(\widetilde{k}_{m-1}, \widetilde{n}_0, \widetilde{n}_1, \ldots, \widetilde{n}_{m-1}, L_1, L_2, \ldots, L_{m-1}\bigr)$$

$$r_{m-1,0} = r_{m-1,0}(\widetilde{k}) = r_{m-1,0}\bigl(\widetilde{k}_{m-1}, \widetilde{n}_0, \widetilde{n}_1, \ldots, \widetilde{n}_{m-1}, L_1, L_2, \ldots, L_{m-1}\bigr)$$

From the previous section, we know that

$$t_{0,1}(\widetilde{k}) = \frac{2\widetilde{n}_0}{\widetilde{n}_0+\widetilde{n}_1}\exp\left[\frac{i\widetilde{k}_0L_1(\widetilde{n}_1-\widetilde{n}_0)}{\widetilde{n}_0}\right] \quad (12)$$

$$r_{0,1}(\widetilde{k}) = \frac{\widetilde{n}_0-\widetilde{n}_1}{\widetilde{n}_0+\widetilde{n}_1}\exp\left[-2i\widetilde{k}_0L_1\right] \quad (13)$$

$$t_{1,0}(\widetilde{k}) = \frac{2\widetilde{n}_1}{\widetilde{n}_0+\widetilde{n}_1}\exp\left[\frac{i\widetilde{k}_1L_1(\widetilde{n}_0-\widetilde{n}_1)}{\widetilde{n}_1}\right] \quad (14)$$

$$r_{1,0}(\widetilde{k}) = \frac{\widetilde{n}_1-\widetilde{n}_0}{\widetilde{n}_1+\widetilde{n}_0}\exp\left[-2i\widetilde{k}_1L_1\right] \quad (15)$$

Computing $t_{0,m-1}$

Let us compute $t_{0,m-1}$ for $m \geq 3$ assuming that $t_{0,m-2}$, $r_{0,m-2}$, $t_{m-2,0}$, $r_{m-2,0}$ have already been computed.

Consider an incident wave $\widetilde{E}_0\exp[i(\omega t-\widetilde{k}_0z)]$ in layer $\widetilde{n}_0$, defined for $z<L_1$. The transmitted wave in $z>L_{m-1}$ will be the sum of an infinite number of "small-waves" resulting from partial transmission and partial reflection at the interfaces. The k-coefficient of all these transmitted small-waves will be given by

$$k \text{ of the "small-waves"} = \frac{\widetilde{k}_0\widetilde{n}_{m-1}}{\widetilde{n}_0}$$

The E-coefficient of the first small-wave comes from a direct transmission from layer $\widetilde{n}_0$ to layer $\widetilde{n}_{m-2}$ (through L_1, L_2, L_{m-2}) and, finally transmission through $z=L_{m-1}$. Therefore,

$$\begin{aligned}&E \text{ of the 1st small-wave}\\ &= t_{0,m-2}\widetilde{E}_0\frac{2\widetilde{n}_{m-2}}{\widetilde{n}_{m-2}+\widetilde{n}_{m-1}}\\ &\quad\times\exp\left[i\widetilde{k}_0L_{m-1}\frac{\widetilde{n}_{m-2}}{\widetilde{n}_0}\left(\frac{\widetilde{n}_{m-1}}{\widetilde{n}_{m-2}}-1\right)\right]\end{aligned}$$

The E-coefficient of the second small-wave comes from calculating the transmission from layer $\widetilde{n}_0$ to layer $\widetilde{n}_{m-2}$ (through L_1, L_2, L_{m-2}) [reflection in $z=L_{m-1}$, reflection in $[L_{m-2},\ldots,L_1]$] and, finally, transmission through $z=L_{m-1}$.

Therefore,

$$\begin{aligned}&E \text{ of the 2nd small-wave}\\ &= t_{0,m-2}\widetilde{E}_0\left\{\frac{\widetilde{n}_{m-2}-\widetilde{n}_{m-1}}{\widetilde{n}_{m-2}+\widetilde{n}_{m-1}}\exp\left[-2i\frac{\widetilde{k}_0\widetilde{n}_{m-2}}{\widetilde{n}_0}L_{m-1}\right]\right.\\ &\qquad\left.\times r_{m-2,0}\left(-\frac{\widetilde{k}_0\widetilde{n}_{m-2}}{\widetilde{n}_0}\right)\right\}\\ &\quad\times\frac{2\widetilde{n}_{m-2}}{\widetilde{n}_{m-2}+\widetilde{n}_{m-1}}\exp\left[\frac{i\widetilde{k}_0L_{m-1}(\widetilde{n}_{m-1}-\widetilde{n}_{m-2})}{\widetilde{n}_0}\right]\end{aligned}$$

Proceeding in the same way for all $\nu>2$, we have

$$\begin{aligned}&E \text{ of the } \nu\text{th small-wave}\\ &= t_{0,m-2}\widetilde{E}_0\left\{\frac{\widetilde{n}_{m-2}-\widetilde{n}_{m-1}}{\widetilde{n}_{m-2}+\widetilde{n}_{m-1}}\exp\left[-2i\frac{\widetilde{k}_0\widetilde{n}_{m-2}}{\widetilde{n}_0}L_{m-1}\right]\right.\\ &\qquad\left.\times r_{m-2,0}\left(-\frac{\widetilde{k}_0\widetilde{n}_{m-2}}{\widetilde{n}_0}\right)\right\}^{\nu-1}\\ &\quad\times\frac{2\widetilde{n}_{m-2}}{\widetilde{n}_{m-2}+\widetilde{n}_{m-1}}\exp\left[\frac{i\widetilde{k}_0L_{m-1}(\widetilde{n}_{m-1}-\widetilde{n}_{m-2})}{\widetilde{n}_0}\right]\end{aligned}$$

Adding all the above small-waves, we obtain

$$\begin{aligned}&t_{0,m-2}E_0\frac{2\widetilde{n}_{m-2}}{\widetilde{n}_{m-2}+\widetilde{n}_{m-1}}\exp\left[\frac{i\widetilde{k}_0L_{m-1}(\widetilde{n}_{m-1}-\widetilde{n}_{m-2})}{\widetilde{n}_0}\right]\\ &\quad\times\left\{1-\frac{\widetilde{n}_{m-2}-\widetilde{n}_{m-1}}{\widetilde{n}_{m-2}+\widetilde{n}_{m-1}}\exp\left[-2i\frac{\widetilde{k}_0\widetilde{n}_{m-2}}{\widetilde{n}_0}L_{m-1}\right]\right.\\ &\qquad\left.\times r_{m-1,0}\left(-\frac{\widetilde{k}_0\widetilde{n}_{m-2}}{\widetilde{n}_0}\right)\right\}^{-1}\end{aligned}$$

Therefore,

$$\begin{aligned}t_{0,m-1} &= t_{0,m-1}(\widetilde{k})\\ &= t_{0,m-2}\frac{2\widetilde{n}_{m-2}}{\widetilde{n}_{m-2}+\widetilde{n}_{m-1}}\exp\left[\frac{i\widetilde{k}_0L_{m-1}(\widetilde{n}_{m-1}-\widetilde{n}_{m-2})}{\widetilde{n}_0}\right]\\ &\quad\times\left\{1-\frac{\widetilde{n}_{m-2}-\widetilde{n}_{m-1}}{\widetilde{n}_{m-2}+\widetilde{n}_{m-1}}\exp\left[-2i\frac{\widetilde{k}_0\widetilde{n}_{m-2}}{\widetilde{n}_0}L_{m-1}\right]\right.\\ &\qquad\left.\times r_{m-2,0}\left(-\frac{\widetilde{k}_0\widetilde{n}_{m-2}}{\widetilde{n}_0}\right)\right\}^{-1} \quad (16)\end{aligned}$$

A brief explanation on notation becomes necessary. When we write, for example, $r_{m-2,0}(-(\widetilde{k}_0\widetilde{n}_{m-2}/\widetilde{n}_0))$, this means "the function $r_{m-2,0}$ applied on $-(\widetilde{k}_0\widetilde{n}_{m-2}/\widetilde{n}_0)$." When we write $t_{0,m-2}$, this means $t_{0,m-2}(\widetilde{k})$. When, say, t_{ij} is used without argument, it means $t_{ij}(\widetilde{k})$. Otherwise the argument is explicitly stated, as in the case of $r_{m-2,0}$ in the formula above.

Computing $r_{0,m-1}$

Assume, again, that the incident wave $\widetilde{E}_0\exp[i(\omega t-\widetilde{k}_0z)]$ is defined for $z<L_1$. The reflection in $[L_1,L_2,\ldots,L_{m-1}]$ generates a reflected wave, also defined in $z<L_1$. This wave is the sum of an infinite number of "small-waves" and an additional wave called here the zeroth-wave. The k-coefficient of all these waves is $-\widetilde{k}_0$.

The zeroth-wave is the first reflection of the incident wave at $[L_1,\ldots,L_{m-1}]$, so

$$E \text{ of the 0th wave} = r_{0,m-2}(\widetilde{k}_0)\widetilde{E}_0$$

The E-coefficient of the first small-wave comes from transmission through $L_1,\ldots,L_{m-2}$, followed by reflection at $z=L_{m-1}$ and, finally, transmission through $L_{m-2},\ldots,L_1$. So,

$$\begin{aligned}&E \text{ of the 1st small-wave}\\ &= t_{0,m-2}\widetilde{E}_0\frac{\widetilde{n}_{m-2}-\widetilde{n}_{m-1}}{\widetilde{n}_{m-2}+\widetilde{n}_{m-1}}\exp\left[-2i\frac{\widetilde{k}_0\widetilde{n}_{m-2}}{\widetilde{n}_0}L_{m-1}\right]\\ &\quad\times t_{m-2,0}\left(-\frac{\widetilde{k}_0\widetilde{n}_{m-2}}{\widetilde{n}_0}\right)\end{aligned}$$

The E-coefficient of the second small-wave comes from transmission through $L_1,\ldots,L_{m-2}$, followed by reflection at $z=L_{m-1}$ [then reflection at $[L_{m-2},\ldots,L_1]$, then reflection

at $z = L_{m-1}$] and, finally, transmission through $L_{m-2}, \ldots, L_1$. So,

$$
\begin{aligned}
&E \text{ of the 2nd small-wave} \\
&\quad = t_{0,m-2}\widetilde{E}_0 \frac{\widetilde{n}_{m-2}-\widetilde{n}_{m-1}}{\widetilde{n}_{m-2}+\widetilde{n}_{m-1}} \exp\left[-2i\frac{\widetilde{k}_0\widetilde{n}_{m-2}}{\widetilde{n}_0}L_{m-1}\right] \\
&\qquad \times \left\{ r_{m-2,0}\left(-\frac{\widetilde{k}_0\widetilde{n}_{m-2}}{\widetilde{n}_0}\right)\frac{\widetilde{n}_{m-2}-\widetilde{n}_{m-1}}{\widetilde{n}_{m-2}+\widetilde{n}_{m-1}} \right. \\
&\qquad\quad \left. \times \exp\left[-2i\frac{\widetilde{k}_0\widetilde{n}_{m-2}}{\widetilde{n}_0}L_{m-1}\right]\right\} t_{m-2,0}\left(-\frac{\widetilde{k}_0\widetilde{n}_{m-2}}{\widetilde{n}_0}\right)
\end{aligned}
$$

So far, the E-coefficient of the νth small-wave comes from transmission through $L_1, \ldots, L_{m-2}$, then reflection at $z = L_{m-1}$ [then reflection at $[L_{m-2}, \ldots, L_1]$, then reflection at $z = L_{m-1}$] $\nu - 1$ times and, finally, transmission through $L_{m-2}, \ldots, L_1$. So,

$$
\begin{aligned}
&E \text{ of the } \nu\text{th small-wave} \\
&\quad = t_{0,m-2}\widetilde{E}_0 \frac{\widetilde{n}_{m-2}-\widetilde{n}_{m-1}}{\widetilde{n}_{m-2}+\widetilde{n}_{m-1}} \exp\left[-2i\frac{\widetilde{k}_0\widetilde{n}_{m-2}}{\widetilde{n}_0}L_{m-1}\right] \\
&\qquad \times \left\{ r_{m-2,0}\left(-\frac{\widetilde{k}_0\widetilde{n}_{m-2}}{\widetilde{n}_0}\right)\frac{\widetilde{n}_{m-2}-\widetilde{n}_{m-1}}{\widetilde{n}_{m-2}+\widetilde{n}_{m-1}} \right. \\
&\qquad\quad \left. \times \exp\left[-2i\frac{\widetilde{k}_0\widetilde{n}_{m-2}}{\widetilde{n}_0}L_{m-1}\right]\right\}^{\nu-1} t_{m-2,0}\left(-\frac{\widetilde{k}_0\widetilde{n}_{m-2}}{\widetilde{n}_0}\right)
\end{aligned}
$$

Therefore, the E-coefficient of the reflected wave defined in $z < L_1$ is

$$
\begin{aligned}
&r_{0,m-2}(\widetilde{k})\widetilde{E}_0 + t_{0,m-2}\widetilde{E}_0 \frac{\widetilde{n}_{m-2}-\widetilde{n}_{m-1}}{\widetilde{n}_{m-2}+\widetilde{n}_{m-1}} \\
&\quad \times \exp\left[-2i\frac{\widetilde{k}_0\widetilde{n}_{m-2}}{\widetilde{n}_0}L_{m-1}\right] t_{m-2,0}\left(-\frac{\widetilde{k}_0\widetilde{n}_{m-2}}{\widetilde{n}_0}\right) \\
&\quad \times \left\{ 1 - r_{m-2,0}\left(-\frac{\widetilde{k}_0\widetilde{n}_{m-2}}{\widetilde{n}_0}\right)\frac{\widetilde{n}_{m-2}-\widetilde{n}_{m-1}}{\widetilde{n}_{m-2}+\widetilde{n}_{m-1}} \right. \\
&\qquad \left. \times \exp\left[-2i\frac{\widetilde{k}_0\widetilde{n}_{m-2}}{\widetilde{n}_0}L_{m-1}\right]\right\}^{-1}
\end{aligned}
$$

So,

$$
\begin{aligned}
r_{0,m-1}(\widetilde{k}) \;=\; & r_{0,m-2}(\widetilde{k}) + t_{0,m-2}\frac{\widetilde{n}_{m-2}-\widetilde{n}_{m-1}}{\widetilde{n}_{m-2}+\widetilde{n}_{m-1}} \\
& \times \exp\left[-2i\frac{\widetilde{k}_0\widetilde{n}_{m-2}}{\widetilde{n}_0}L_{m-1}\right] t_{m-2,0}\left(-\frac{\widetilde{k}\widetilde{n}_{m-2}}{\widetilde{n}_0}\right) \\
& \times \left\{ 1 - r_{m-2,0}\left(-\frac{\widetilde{k}_0\widetilde{n}_{m-2}}{\widetilde{n}_0}\right)\frac{\widetilde{n}_{m-2}-\widetilde{n}_{m-1}}{\widetilde{n}_{m-2}+\widetilde{n}_{m-1}} \right. \\
& \left. \times \exp\left[-2i\frac{\widetilde{k}_0\widetilde{n}_{m-2}}{\widetilde{n}_0}L_{m-1}\right]\right\}^{-1} \qquad (17)
\end{aligned}
$$

Computing $t_{m-1,0}$

Assume that the wave $\widetilde{E}_{m-1}\exp[i(\omega t + \widetilde{k}_{m-1}z)]$ is defined for $z > L_{m-1}$, where the refraction index is $\widetilde{n}_{m-1}$ (see Fig. 6). The k-coefficient of the transmitted wave defined for $z < L_1$, as well as the k-coefficient of all the small-waves whose addition is the transmitted wave, will be $\widetilde{k}_{m-1}\widetilde{n}_0/\widetilde{n}_{m-1}$.

As in the previous cases, the transmitted wave is the sum of infinitely many small-waves.

The E-coefficient of the first small-wave is obtained by transmission through $z = L_{m-1}$ (from "right" to "left") followed by transmission through $[L_{m-2}, \ldots, L_1]$. So,

$$
\begin{aligned}
&E \text{ of the 1st small-wave} \\
&\quad = \widetilde{E}_{m-1}\frac{2\widetilde{n}_{m-1}}{\widetilde{n}_{m-1}+\widetilde{n}_{m-2}} \exp\left[\frac{i\widetilde{k}_{m-1}L_{m-1}(\widetilde{n}_{m-2}-\widetilde{n}_{m-1})}{\widetilde{n}_{m-1}}\right] \\
&\qquad \times t_{m-2,0}\left(\frac{\widetilde{k}_{m-1}\widetilde{n}_{m-2}}{\widetilde{n}_{m-1}}\right)
\end{aligned}
$$

The E-coefficient of the second small-wave is obtained by transmission through L_{m-1} (from right to left), followed by [reflection at $[L_{m-2}, \ldots, L_1]$, reflection at $z = L_{m-1}$] and, finally, transmission through $[L_{m-2}, \ldots, L_1]$. So,

$$
\begin{aligned}
&E \text{ of the 2nd small-wave} \\
&\quad = \widetilde{E}_{m-1}\frac{2\widetilde{n}_{m-1}}{\widetilde{n}_{m-1}+\widetilde{n}_{m-2}} \exp\left[\frac{i\widetilde{k}_{m-1}L_{m-1}(\widetilde{n}_{m-2}-\widetilde{n}_{m-1})}{\widetilde{n}_{m-1}}\right] \\
&\qquad \times r_{m-2,0}\left(\frac{\widetilde{n}_{m-2}\widetilde{k}_{m-1}}{\widetilde{n}_{m-1}}\right)\frac{\widetilde{n}_{m-2}-\widetilde{n}_{m-1}}{\widetilde{n}_{m-2}+\widetilde{n}_{m-1}} \\
&\qquad \times \exp\left(\frac{2i\widetilde{k}_{m-1}\widetilde{n}_{m-2}L_{m-1}}{\widetilde{n}_{m-1}}\right) t_{m-2,0}\left(\frac{\widetilde{k}_{m-1}\widetilde{n}_{m-2}}{\widetilde{n}_{m-1}}\right)
\end{aligned}
$$

The E-coefficient of the νth small-wave is obtained by transmission through L_{m-1} (from right to left), followed by [reflection at $[L_{m-2}, \ldots, L_1]$, reflection at $z = L_{m-1}$] $\nu - 1$ times, and finally, transmission through $[L_{m-2}, \ldots, L_1]$. So,

$$
\begin{aligned}
&E \text{ of the } \nu\text{th small-wave} \\
&\quad = \widetilde{E}_{m-1}\frac{2\widetilde{n}_{m-1}}{\widetilde{n}_{m-1}+\widetilde{n}_{m-2}} \exp\left[\frac{i\widetilde{k}_{m-1}L_{m-1}(\widetilde{n}_{m-2}-\widetilde{n}_{m-1})}{\widetilde{n}_{m-1}}\right] \\
&\qquad \times \left\{ r_{m-2,0}\left(\frac{\widetilde{n}_{m-2}\widetilde{k}_{m-1}}{\widetilde{n}_{m-1}}\right)\frac{\widetilde{n}_{m-2}-\widetilde{n}_{m-1}}{\widetilde{n}_{m-2}+\widetilde{n}_{m-1}} \right. \\
&\qquad\quad \left. \times \exp\left(\frac{2i\widetilde{k}_{m-1}\widetilde{n}_{m-2}L_{m-1}}{\widetilde{n}_{m-1}}\right)\right\}^{\nu-1} t_{m-1,1}\left(\frac{\widetilde{k}_{m-1}\widetilde{n}_{m-2}}{\widetilde{n}_{m-1}}\right)
\end{aligned}
$$

Adding all the small-waves, we obtain

$$
\begin{aligned}
&E \text{ of the transmitted wave in } z < L_1 \\
&\quad = \widetilde{E}_{m-1}\frac{2\widetilde{n}_{m-1}}{\widetilde{n}_{m-1}+\widetilde{n}_{m-2}} \exp\left[\frac{i\widetilde{k}_{m-1}L_{m-1}(\widetilde{n}_{m-2}-\widetilde{n}_{m-1})}{\widetilde{n}_{m-1}}\right] \\
&\qquad \times t_{m-2,0}\left(\frac{\widetilde{k}_{m-1}\widetilde{n}_{m-2}}{\widetilde{n}_{m-1}}\right) \\
&\qquad \times \left\{ 1 - r_{m-2,0}\left(\frac{\widetilde{n}_{m-2}\widetilde{k}_{m-1}}{\widetilde{n}_{m-1}}\right)\frac{\widetilde{n}_{m-2}-\widetilde{n}_{m-1}}{\widetilde{n}_{m-2}+\widetilde{n}_{m-1}} \right. \\
&\qquad\quad \left. \times \exp\left(\frac{2i\widetilde{k}_{m-1}\widetilde{n}_{m-2}L_{m-1}}{\widetilde{n}_{m-1}}\right)\right\}^{-1}
\end{aligned}
$$

Therefore,

$$t_{m-1,0}(\widetilde{k}) = \frac{2\widetilde{n}_{m-1}}{\widetilde{n}_{m-1}+\widetilde{n}_{m-2}} \exp\left[\frac{i\widetilde{k}_{m-1}L_{m-1}(\widetilde{n}_{m-2}-\widetilde{n}_{m-1})}{\widetilde{n}_{m-1}}\right] \times t_{m-2,0}\left(\frac{\widetilde{k}_{m-1}\widetilde{n}_{m-2}}{\widetilde{n}_{m-1}}\right) \times \left\{1 - r_{m-2,0}\left(\frac{\widetilde{n}_{m-2}\widetilde{k}_{m-1}}{\widetilde{n}_{m-1}}\right)\frac{\widetilde{n}_{m-2}-\widetilde{n}_{m-1}}{\widetilde{n}_{m-2}+\widetilde{n}_{m-1}} \times \exp\left(\frac{2i\widetilde{k}_{m-1}\widetilde{n}_{m-2}L_{m-1}}{\widetilde{n}_{m-1}}\right)\right\}^{-1} \quad (18)$$

Computing $r_{m-1,0}(\widetilde{k})$

Assume, again, that the incident wave $\widetilde{E}_{m-1}\exp[i(\omega t+\widetilde{k}_{m-1}z)]$ is defined for $z > L_{m-1}$. We wish to compute the reflected wave defined, also, in the layer $\widetilde{n}_{m-1}$. The k-coefficient, as always, will be $-\widetilde{k}_{m-1}$. The reflected wave we wish to compute is the sum of infinitely many small-waves plus a zeroth-wave.

The zeroth-wave is the reflection of the incident wave at $z = L_{m-1}$. So,

$$E \text{ of the 0th wave} = \widetilde{E}_{m-1}\frac{\widetilde{n}_{m-1}-\widetilde{n}_{m-2}}{\widetilde{n}_{m-1}+\widetilde{n}_{m-2}}\exp\left(-2i\widetilde{k}_{m-1}L_{m-1}\right)$$

The first small-wave comes from transmission from right to left through $z = L_{m-1}$, followed by reflection at $[L_{m-2}, \ldots, L_1]$, followed by transmission from left to right through $z = L_{m-1}$. So,

$$E \text{ of the 1st small-wave} = \widetilde{E}_{m-1}\frac{2\widetilde{n}_{m-1}}{\widetilde{n}_{m-1}+\widetilde{n}_{m-2}}\exp\left[\frac{i\widetilde{k}_{m-1}L_{m-1}(\widetilde{n}_{m-2}-\widetilde{n}_{m-1})}{\widetilde{n}_{m-1}}\right] \times r_{m-2,0}\left(\frac{\widetilde{k}_{m-1}\widetilde{n}_{m-2}}{\widetilde{n}_{m-1}}\right) \times \frac{2\widetilde{n}_{m-2}}{\widetilde{n}_{m-2}+\widetilde{n}_{m-1}}\exp\left[-i\widetilde{k}_{m-1}L_{m-1}\frac{\widetilde{n}_{m-2}}{\widetilde{n}_{m-1}}\frac{\widetilde{n}_{m-1}-\widetilde{n}_{m-2}}{\widetilde{n}_{m-2}}\right]$$

The second small-wave comes from transmission from right to left through $z = L_{m-1}$, then reflection at $[L_{m-2}, \ldots, L_1]$, then [reflection at $z = L_{m-1}$, reflection at $[L_{m-2}, \ldots, L_1]$] and, finally, transmission (left–right) through $z = L_{m-1}$. So,

$$E \text{ of the 2nd small-wave} = \widetilde{E}_{m-1}\frac{2\widetilde{n}_{m-1}}{\widetilde{n}_{m-1}+\widetilde{n}_{m-2}}\exp\left[\frac{i\widetilde{k}_{m-1}L_{m-1}(\widetilde{n}_{m-2}-\widetilde{n}_{m-1})}{\widetilde{n}_{m-1}}\right] \times r_{m-2,0}\left(\frac{\widetilde{k}_{m-1}\widetilde{n}_{m-2}}{\widetilde{n}_{m-1}}\right) \times \frac{\widetilde{n}_{m-2}-\widetilde{n}_{m-1}}{\widetilde{n}_{m-2}+\widetilde{n}_{m-1}}\exp\left(\frac{2i\widetilde{k}_{m-1}\widetilde{n}_{m-2}L_{m-1}}{\widetilde{n}_{m-1}}\right) \times r_{m-1,1}\left(\frac{\widetilde{k}_{m-1}\widetilde{n}_{m-2}}{\widetilde{n}_{m-1}}\right) \times \frac{2\widetilde{n}_{m-2}}{\widetilde{n}_{m-2}+\widetilde{n}_{m-1}}\exp\left[-i\widetilde{k}_{m-1}L_{m-1}\frac{\widetilde{n}_{m-1}-\widetilde{n}_{m-2}}{\widetilde{n}_{m-1}}\right]$$

The νth small-wave comes from transmission (right–left) through $z = L_{m-1}$, then reflection at $[L_{m-2}, \ldots, L_1]$, then [reflection at $z = L_{m-1}$, reflection at $[L_{m-2}, \ldots, L_1]$] $\nu-1$ times, and, finally, transmission left–right through $z = L_{m-1}$. So,

$$E \text{ of the } \nu\text{th small-wave} = \widetilde{E}_{m-1}\frac{2\widetilde{n}_{m-1}}{\widetilde{n}_{m-1}+\widetilde{n}_{m-2}}\exp\left[\frac{i\widetilde{k}_{m-1}L_{m-1}(\widetilde{n}_{m-2}-\widetilde{n}_{m-1})}{\widetilde{n}_{m-1}}\right] \times r_{m-2,0}\left(\frac{\widetilde{k}_{m-1}\widetilde{n}_{m-2}}{\widetilde{n}_{m-1}}\right) \times \left\{\frac{\widetilde{n}_{m-2}-\widetilde{n}_{m-1}}{\widetilde{n}_{m-2}+\widetilde{n}_{m-1}}\exp\left(\frac{2i\widetilde{k}_{m-1}L_{m-1}\widetilde{n}_{m-2}}{\widetilde{n}_{m-1}}\right) \times r_{m-2,0}\left(\frac{\widetilde{k}_{m-1}\widetilde{n}_{m-2}}{\widetilde{n}_{m-1}}\right)\right\}^{\nu-1} \times \frac{2\widetilde{n}_{m-2}}{\widetilde{n}_{m-2}+\widetilde{n}_{m-1}}\exp\left[-i\widetilde{k}_{m-1}L_{m-1}\frac{\widetilde{n}_{m-1}-\widetilde{n}_{m-2}}{\widetilde{n}_{m-1}}\right]$$

Adding all these waves, we obtain

$$E \text{ of the reflected wave in } z > L_{m-1} = \widetilde{E}_{m-1}\frac{\widetilde{n}_{m-1}-\widetilde{n}_{m-2}}{\widetilde{n}_{m-1}+\widetilde{n}_{m-2}}\exp\left(-2i\widetilde{k}_{m-1}L_{m-1}\right) + \widetilde{E}_{m-1}\frac{2\widetilde{n}_{m-1}}{\widetilde{n}_{m-1}+\widetilde{n}_{m-2}}\exp\left[\frac{i\widetilde{k}_{m-1}L_{m-1}(\widetilde{n}_{m-2}-\widetilde{n}_{m-1})}{\widetilde{n}_{m-1}}\right] \times \left\{1 - \frac{\widetilde{n}_{m-2}-\widetilde{n}_{m-1}}{\widetilde{n}_{m-2}+\widetilde{n}_{m-1}}\exp\left(\frac{2i\widetilde{k}_{m-1}L_{m-1}\widetilde{n}_{m-2}}{\widetilde{n}_{m-1}}\right) \times r_{m-2,0}\left(\frac{\widetilde{k}_{m-1}\widetilde{n}_{m-2}}{\widetilde{n}_{m-1}}\right)\right\}^{-1} \times r_{m-2,0}\left(\frac{\widetilde{k}_{m-1}\widetilde{n}_{m-2}}{\widetilde{n}_{m-1}}\right)\frac{2\widetilde{n}_{m-2}}{\widetilde{n}_{m-2}+\widetilde{n}_{m-1}} \times \exp\left[-i\widetilde{k}_{m-1}L_{m-1}\frac{\widetilde{n}_{m-1}-\widetilde{n}_{m-2}}{\widetilde{n}_{m-1}}\right]$$

So,

$$r_{m-1,0}(\widetilde{k}_{m-1}) = \frac{\widetilde{n}_{m-1}-\widetilde{n}_{m-2}}{\widetilde{n}_{m-1}+\widetilde{n}_{m-2}}\exp\left(-2i\widetilde{k}_{m-1}L_{m-1}\right) + \frac{2\widetilde{n}_{m-1}}{\widetilde{n}_{m-1}+\widetilde{n}_{m-2}}\exp\left[\frac{i\widetilde{k}_{m-1}L_{m-1}(\widetilde{n}_{m-2}-\widetilde{n}_{m-1})}{\widetilde{n}_{m-1}}\right] \times \left\{1 - \frac{\widetilde{n}_{m-2}-\widetilde{n}_{m-1}}{\widetilde{n}_{m-2}+\widetilde{n}_{m-1}}\exp\left(\frac{2i\widetilde{k}_{m-1}L_{m-1}\widetilde{n}_{m-2}}{\widetilde{n}_{m-1}}\right) \times r_{m-2,0}\left(\frac{\widetilde{k}_{m-1}\widetilde{n}_{m-2}}{\widetilde{n}_{m-1}}\right)\right\}^{-1} \times r_{m-2,0}\left(\frac{\widetilde{k}_{m-1}\widetilde{n}_{m-2}}{\widetilde{n}_{m-1}}\right)\frac{2\widetilde{n}_{m-2}}{\widetilde{n}_{m-2}+\widetilde{n}_{m-1}} \times \exp\left[-i\widetilde{k}_{m-1}L_{m-1}\frac{\widetilde{n}_{m-1}-\widetilde{n}_{m-2}}{\widetilde{n}_{m-1}}\right]$$

Thus,

$$
\begin{aligned}
&r_{m-1,0}(\widetilde{k}_{m-1})\\
&\quad=\frac{\widetilde{n}_{m-1}-\widetilde{n}_{m-2}}{\widetilde{n}_{m-1}+\widetilde{n}_{m-2}}\exp\bigl(-2i\widetilde{k}_{m-1}L_{m-1}\bigr)\\
&\qquad+\frac{4\widetilde{n}_{m-1}\widetilde{n}_{m-2}}{(\widetilde{n}_{m-1}+\widetilde{n}_{m-2})^2}\exp\left[\frac{2i\widetilde{k}_{m-1}L_{m-1}(\widetilde{n}_{m-2}-\widetilde{n}_{m-1})}{\widetilde{n}_{m-1}}\right]\\
&\qquad\times r_{m-2,0}\left(\frac{\widetilde{k}_{m-1}\widetilde{n}_{m-2}}{\widetilde{n}_{m-1}}\right)\\
&\qquad\times\left\{1-\frac{\widetilde{n}_{m-2}-\widetilde{n}_{m-1}}{\widetilde{n}_{m-2}+\widetilde{n}_{m-1}}\exp\left(\frac{2i\widetilde{k}_{m-1}L_{m-1}\widetilde{n}_{m-2}}{\widetilde{n}_{m-1}}\right)\right.\\
&\qquad\quad\left.\times r_{m-2,0}\left(\frac{\widetilde{k}_{m-1}\widetilde{n}_{m-2}}{\widetilde{n}_{m-1}}\right)\right\}^{-1}
\end{aligned}
\tag{19}
$$

1.4.3. Organizing the Computations

The analysis of Eqs. (16)–(19) reveals that for computing, say, $t_{0,m-1}(\widetilde{k})$, we need to compute $t_{0,\nu}(\widetilde{k})$ for $\nu < m-1$ and $r_{\nu,0}(-\widetilde{k}\widetilde{n}_{\nu-1}/\widetilde{n}_0)$ for $\nu < m-1$.

Analogously, for computing $r_{0,m-1}(\widetilde{k})$, we need to compute $t_{0,\nu}(\widetilde{k})$ for $\nu < m-1$, $t_{\nu,0}(-\widetilde{k}\widetilde{n}_{\nu-1}/\widetilde{n}_0)$ for $\nu < m-1$, $r_{\nu,0}(-\widetilde{k}\widetilde{n}_{\nu-1}/\widetilde{n}_0)$ for $\nu < m-2$, and $r_{0,\nu}(\widetilde{k})$ for $\nu = m-2$.

Let us see this in the following tables, for $m = 4$. Under the $(j+1)$th column of the table, we write the quantities that are needed to compute the quantities that appear under column j. For example, we read that for computing $t_{0,4}(\widetilde{k})$, we need $t_{0,3}(\widetilde{k})$ and $r_{3,0}(-\widetilde{k}\widetilde{n}_3/\widetilde{n}_0)$, and so on.

Computing Tree of $t_{0,4}(\widetilde{k})$

$t_{0,4}(\widetilde{k})$	$t_{0,3}(\widetilde{k})$	$t_{0,2}(\widetilde{k})$	$t_{0,1}(\widetilde{k})$
		$r_{2,0}(-\widetilde{k}\widetilde{n}_2/\widetilde{n}_0)$	$r_{1,0}(-\widetilde{k}\widetilde{n}_1/\widetilde{n}_0)$
		$r_{2,0}(-\widetilde{k}\widetilde{n}_2/\widetilde{n}_0)$	$r_{1,0}(-\widetilde{k}\widetilde{n}_1/\widetilde{n}_0)$
	$r_{3,0}(-\widetilde{k}\widetilde{n}_3/\widetilde{n}_0)$	$r_{2,0}(-\widetilde{k}\widetilde{n}_2/\widetilde{n}_0)$	$r_{1,0}(-\widetilde{k}\widetilde{n}_1/\widetilde{n}_0)$

Computing Tree of $r_{0,4}(\widetilde{k})$

$r_{0,4}(\widetilde{k})$	$t_{0,3}(\widetilde{k})$	$t_{0,2}(\widetilde{k})$	$t_{0,1}(\widetilde{k})$
			$r_{1,0}(-\widetilde{k}\widetilde{n}_1/\widetilde{n}_0)$
		$r_{2,0}(-\widetilde{k}\widetilde{n}_2/\widetilde{n}_0)$	$r_{1,0}(-\widetilde{k}\widetilde{n}_1/\widetilde{n}_0)$
	$t_{3,0}(-\widetilde{k}\widetilde{n}_3/\widetilde{n}_0)$	$t_{2,0}(-\widetilde{k}\widetilde{n}_2/\widetilde{n}_0)$	$t_{1,0}(-\widetilde{k}\widetilde{n}_1/\widetilde{n}_0)$
			$r_{1,0}(-\widetilde{k}\widetilde{n}_1/\widetilde{n}_0)$
		$r_{2,0}(-\widetilde{k}\widetilde{n}_2/\widetilde{n}_0)$	$r_{1,0}(-\widetilde{k}\widetilde{n}_1/\widetilde{n}_0)$
	$r_{0,3}(\widetilde{k})$	$t_{0,2}(\widetilde{k})$	$t_{0,1}(\widetilde{k})$
			$r_{1,0}(-\widetilde{k}\widetilde{n}_1/\widetilde{n}_0)$
		$t_{2,0}(-\widetilde{k}\widetilde{n}_2/\widetilde{n}_0)$	$t_{1,0}(-\widetilde{k}\widetilde{n}_1/\widetilde{n}_0)$
			$r_{1,0}(-\widetilde{k}\widetilde{n}_1/\widetilde{n}_0)$
		$r_{0,2}(\widetilde{k})$	$t_{0,1}(\widetilde{k})$
			$t_{1,0}(-\widetilde{k}\widetilde{n}_1/\widetilde{n}_0)$
			$r_{0,1}(\widetilde{k})$

Therefore, all the computation can be performed using the following conceptual algorithm.

Algorithm

Step 1. Compute $t_{0,1}(\widetilde{k})$, $r_{0,1}(\widetilde{k})$, $t_{1,0}(-\widetilde{k}\widetilde{n}_1/\widetilde{n}_0)$, $r_{1,0}(-\widetilde{k}\widetilde{n}_1/\widetilde{n}_0)$.

Step 2. For $\nu = 3, \ldots, m-1$,
Compute $t_{0,\nu}(\widetilde{k})$, $r_{0,\nu}(\widetilde{k})$, $t_{\nu,0}(-\widetilde{k}\widetilde{n}_{\nu-1}/\widetilde{n}_0)$, $r_{0,\nu}(-\widetilde{k}\widetilde{n}_{\nu-1}/\widetilde{n}_0)$.

1.4.4. Computation by Matricial Methods

The previous sections provide a practical way of computing transmissions and reflections and understanding how complex waves are generated as summations of simpler ones. In this section, we compute the same parameters using a more compact calculation procedure, although some insight is lost [16]. The assumptions are exactly the ones of the previous sections. In layer $\tilde{n}_\nu$, for $\nu = 0, 1, \ldots, m-1$, we have two waves given by

$$E_T^\nu \exp\bigl[i\bigl(wt-\widetilde{k}_\nu z\bigr)\bigr]$$

and

$$E_R^\nu \exp\bigl[i\bigl(wt+\widetilde{k}_\nu z\bigr)\bigr]$$

The first is a summation of "transmitted small-waves" and the second is a summation of "reflected small-waves." As before, $k = 2\pi/\lambda$,

$$\widetilde{k}_0 = \widetilde{k} \quad \text{and} \quad \widetilde{k}_\nu = \frac{\widetilde{k}\widetilde{n}_\nu}{\tilde{n}_0}$$

for all $\nu = 0, 1, \ldots, m-1$. We can intepret that $E_T^0 \exp[i(wt-\widetilde{k}z)]$ is the "incident wave." Since there are no reflected waves in the last semi-infinite layer, we have that

$$E_R^{m-1} = 0$$

Using the continuity of the waves and their derivatives with respect to x at the interfaces $L_1, \ldots, L_{m-1}$, we get, for $\nu = 1, 2, \ldots, m-1$,

$$
\begin{aligned}
&E_T^{\nu-1}\exp\bigl(-i\widetilde{k}_{\nu-1}L_\nu\bigr)+E_R^{\nu-1}\exp\bigl(i\widetilde{k}_{\nu-1}L_\nu\bigr)\\
&\quad=E_T^\nu\exp\bigl(-i\widetilde{k}_\nu L_\nu\bigr)+E_R^\nu\exp\bigl(i\widetilde{k}_\nu L_\nu\bigr)
\end{aligned}
$$

and

$$
\begin{aligned}
&-\widetilde{k}_{\nu-1}E_T^{\nu-1}\exp\bigl(-i\widetilde{k}_{\nu-1}L_\nu\bigr)+\widetilde{k}_{\nu-1}E_R^{\nu-1}\exp\bigl(i\widetilde{k}_{\nu-1}L_\nu\bigr)\\
&\quad=-\widetilde{k}_\nu E_T^\nu\exp\bigl(-i\widetilde{k}_\nu L_\nu\bigr)+\widetilde{k}_\nu E_R^\nu\exp\bigl(i\widetilde{k}_\nu L_\nu\bigr)
\end{aligned}
$$

In matricial form, and using $\widetilde{k}_\nu = \widetilde{k}\tilde{n}_\nu/\tilde{n}_0$, we obtain

$$
\begin{aligned}
&\begin{pmatrix}1 & 1\\ -\widetilde{n}_{\nu-1} & \widetilde{n}_{\nu-1}\end{pmatrix}\begin{pmatrix}\exp(-i\widetilde{k}_{\nu-1}L_\nu) & 0\\ 0 & \exp(i\widetilde{k}_{\nu-1}L_\nu)\end{pmatrix}\begin{pmatrix}E_T^{\nu-1}\\ E_R^{\nu-1}\end{pmatrix}\\
&\quad=\begin{pmatrix}1 & 1\\ -\widetilde{n}_\nu & \widetilde{n}_\nu\end{pmatrix}\begin{pmatrix}\exp(-i\widetilde{k}_\nu L_\nu) & 0\\ 0 & \exp(i\widetilde{k}_\nu L_\nu)\end{pmatrix}\begin{pmatrix}E_T^\nu\\ E_R^\nu\end{pmatrix}
\end{aligned}
$$

Therefore,

$$\begin{pmatrix} E_T^{\nu} \\ E_R^{\nu} \end{pmatrix} = \begin{pmatrix} \exp(-i\widetilde{k}_{\nu}L_{\nu}) & 0 \\ 0 & \exp(i\widetilde{k}_{\nu}L_{\nu}) \end{pmatrix} \times \frac{1}{2\widetilde{n}_{\nu}} \begin{pmatrix} \widetilde{n}_{\nu}+\widetilde{n}_{\nu-1} & \widetilde{n}_{\nu}-\widetilde{n}_{\nu-1} \\ \widetilde{n}_{\nu}-\widetilde{n}_{\nu-1} & \widetilde{n}_{\nu}+\widetilde{n}_{\nu-1} \end{pmatrix} \times \begin{pmatrix} \exp(-i\widetilde{k}_{\nu-1}L_{\nu}) & 0 \\ 0 & \exp(i\widetilde{k}_{\nu-1}L_{\nu}) \end{pmatrix} \begin{pmatrix} E_T^{\nu-1} \\ E_R^{\nu-1} \end{pmatrix}$$

Let us write, for $\nu = 1, \ldots, m-1$,

$$A_{\nu} = \frac{1}{2\widetilde{n}_{\nu}} \begin{pmatrix} \widetilde{n}_{\nu}+\widetilde{n}_{\nu-1} & \widetilde{n}_{\nu}-\widetilde{n}_{\nu-1} \\ \widetilde{n}_{\nu}-\widetilde{n}_{\nu-1} & \widetilde{n}_{\nu}+\widetilde{n}_{\nu-1} \end{pmatrix}$$

Then,

$$\begin{pmatrix} E_T^{\nu+1} \\ E_R^{\nu+1} \end{pmatrix} = \begin{pmatrix} \exp(-i\widetilde{k}_{\nu+1}L_{\nu+1}) & 0 \\ 0 & \exp(i\widetilde{k}_{\nu+1}L_{\nu+1}) \end{pmatrix} \times A_{\nu+1} \begin{pmatrix} \exp(-i\widetilde{k}_{\nu}[L_{\nu+1}-L_{\nu}]) & 0 \\ 0 & \exp(i\widetilde{k}_{\nu}[L_{\nu+1}-L_{\nu}]) \end{pmatrix} \times A_{\nu} \begin{pmatrix} \exp(-i\widetilde{k}_{\nu-1}L_{\nu}) & 0 \\ 0 & \exp(i\widetilde{k}_{\nu-1}L_{\nu}) \end{pmatrix} \begin{pmatrix} E_T^{\nu-1} \\ E_R^{\nu-1} \end{pmatrix}$$

Let $d_{\nu} \equiv L_{\nu+1} - L_{\nu}$ ($\nu = 1, \ldots, m-2$) be the thickness of layer ν. We define, for $\nu = 1, \ldots, m-2$,

$$M_{\nu} = A_{\nu+1} \begin{pmatrix} \exp(-i\widetilde{k}_{\nu}d_{\nu}) & 0 \\ 0 & \exp(i\widetilde{k}_{\nu}d_{\nu}) \end{pmatrix}$$

Then, setting for simplicity and without loss of generality, $L_1 = 0$,

$$\begin{pmatrix} E_T^{m-1} \\ E_R^{m-1} \end{pmatrix} = \begin{pmatrix} \exp(i\widetilde{k}_{m-1}L_{m-1}) & 0 \\ 0 & \exp(i\widetilde{k}_{m-1}L_{m-1}) \end{pmatrix} M_{m-2} \times \cdots \times M_1 A_1 \begin{pmatrix} E_T^0 \\ E_R^0 \end{pmatrix}$$

Define

$$M = M_{m-2} \times \cdots \times M_1 A_1 = \begin{pmatrix} M_{11} & M_{12} \\ M_{21} & M_{22} \end{pmatrix}$$

and

$$M' = \begin{pmatrix} \exp(i\widetilde{k}_{m-1}L_{m-1}) & 0 \\ 0 & \exp(i\widetilde{k}_{m-1}L_{m-1}) \end{pmatrix} M = \begin{pmatrix} M'_{11} & M'_{12} \\ M'_{21} & M'_{22} \end{pmatrix}$$

Using $E_R^{m-1} = 0$, we obtain that

$$E_R^0 = -\frac{M'_{21}}{M'_{22}} E_T^0 = -\frac{M_{21}}{M_{22}} E_T^0$$

and

$$E_T^{m-1} = \left(M'_{11} - \frac{M'_{12}M'_{21}}{M'_{22}}\right) E_T^0 = \exp\left(i\widetilde{k}_{m-1}L_{m-1}\right)\left(M_{11} - \frac{M_{12}M_{21}}{M_{22}}\right) E_T^0$$

So,

$$r_{0,m-1} = -\frac{M_{21}}{M_{22}}$$

and

$$t_{0,m-1} = \exp\left(i\widetilde{k}_{m-1}L_{m-1}\right)\left(M_{11} - \frac{M_{12}M_{21}}{M_{22}}\right) \tag{20}$$

In this deduction, we assumed that the transmitted wave in the final layer n_{m-1} is $E_T^{m-1}\exp[i(wt - \widetilde{k}_{m-1}z)]$. For this reason, the factor $\exp(i\widetilde{k}_{m-1}L_{m-1})$ appeared in the final computation of $t_{1,m-1}$. In other words, according to (20), the transmitted wave in the final layer is

$$\left(M_{11} - \frac{M_{12}M_{21}}{M_{22}}\right) E_T^0 \exp\left[i\left(wt - \widetilde{k}_{m-1}\left(z - L_{m-1}\right)\right)\right]$$

For energy computations, since $|\exp(i\widetilde{k}_{m-1}L_{m-1})| = 1$, the presence of this factor in the computation of $t_{0,m-1}$ is irrelevant.

1.4.5. Transmitted and Reflected Energy

Assume that the layers $z < L_1$ and $z > L_{m-1}$ are transparent. In this case, the coefficients n_0 and n_{m-1} are real, so we have

$$\text{incident energy} = n_0|\widetilde{E}|^2$$

$$\text{transmitted energy} = n_{m-1}|E\text{-coefficient of the transmitted wave}|^2$$

and

$$\text{reflected energy} = n_0|E\text{-coefficient of the reflected wave}|^2$$

Accordingly, we define

$$\text{transmittance} = \frac{\text{trasmitted energy}}{\text{incident energy}}$$

and

$$\text{reflectance} = \frac{\text{reflected energy}}{\text{incident energy}}$$

In other words,

$$\text{transmittance} = \frac{n_{m-1}}{n_0}|t_{0,m-1}|^2 \tag{21}$$

and

$$\text{reflectance} = |r_{0,m-1}|^2 \tag{22}$$

If *all* the layers were transparent, we would necessarily have that

$$\text{incident energy} = \text{transmitted energy} + \text{reflected energy}$$

and, in that case:

$$\text{transmittance} + \text{ reflectance} = 1$$

Assume now that the layer $L_{m-2} < z < L_{m-1}$ is also transparent, so that $\widetilde{n}_{m-2}$ is also real. Consider the transmission coefficient $t_{0,m-1}$ as a function of L_{m-1}, keeping fixed all the other arguments. By (16), we see that $|t_{0,m-1}|^2$ is periodic and that its period is $\lambda n_0/(2n_{m-2})$.

Assume now that all the layers are transparent and, without loss of generality, $L_1 = 0$. We consider $|t_{0,m-1}|^2$ as a function of the thicknesses $d_1 \equiv L_2 - L_1, \ldots, d_{m-2} \equiv L_{m-1} - L_{m-2}$. As above, it can be seen that $|t_{0,m-1}|^2$ is periodic with respect to each of the above variables, and that its period with respect to d_i $(i = 1, 2, \ldots, m-2)$ is $\lambda n_0/(2n_i)$.

1.5. Nonnormal Incidence and Linear-System Computations

In the previous section, we deduced explicit formulae for transmitted and reflected energies when light impinges normally to the surface of the layers. Explicit formulae are important because they help to understand how waves effectively behave. However, it is perhaps simpler to perform computations using an implicit representation of transmitted and reflected waves inside each layer. As we are going to see, in this way the electric and magnetic vectors arise as solutions of a single linear system of equations. This approach allows us to deal in a rather simple way with a more involved situation: the case in which the incidence is not normal, so that the plane of propagation is not parallel to the interfaces. The case considered in the previous section is a particular case of this.

Assume that, in the three-dimensional space xyz, we have m layers divided by the interface planes $z = L_1, \ldots, z = L_{m-1}$ and characterized by the complex refraction indices $\widetilde{n}_0, \ldots, \widetilde{n}_{m-1}$. Therefore, we have, for $\nu = 0, 1, \ldots, m-1$,

$$\widetilde{n}_\nu = n_\nu - i\kappa_\nu$$

where, as always, n_ν represents the real refraction index and κ_ν is the attenuation coefficient. We assume that $\kappa_0 = \kappa_{m-1} = 0$, so the first and last layer are transparent.

Suppose that light arrives at the first surface $z = L_1$ with an angle θ_0 with respect to the normal to the surface. This means that the vector of propagation of the incident light in the first layer is

$$\mathbf{s}_0 = \big(\sin(\theta_0), 0, \cos(\theta_0)\big)$$

Accordingly (for example, invoking Snell's law), the angle with the normal of the transmitted wave in layer ν is

$$\theta_\nu = \frac{n_\nu}{n_0}\sin(\theta_0)$$

and, consequently, the vector of propagation of the transmitted wave in the layer ν will be

$$\mathbf{s}_\nu = \big(\sin(\theta_\nu), 0, \cos(\theta_\nu)\big)$$

Reflected waves are generated in the layers $0, 1, \ldots, m-2$. By Snell's laws, their vectors of propagation are $(\sin(\theta_\nu), 0, -\cos(\theta_\nu))$ for $\nu = 0, 1, \ldots, m-2$.

Incident light in layer n_0 is represented by the electric vector $\mathbf{E}$ and the magnetic vector $\mathbf{H}$. Electromagnetic theory [8] tells that both $\mathbf{E}$ and $\mathbf{H}$ are orthogonal to $\mathbf{s_0}$. Moreover, the relation between these vectors is

$$\mathbf{H} = n_0\mathbf{s}_0 \times \mathbf{E} \tag{23}$$

where $\times$ denotes the vectorial product. We consider that the electromagnetic vectors are linearly polarized, so the considerations above lead to the following expression for $\mathbf{E}$:

$$\begin{aligned}\mathbf{E} = {} & \big(-E_p\cos(\theta_0), E_y, E_p\sin(\theta_0)\big) \\ & \times \exp\big\{i\big[\omega t - k\big(x\sin(\theta_0) + z\cos(\theta_0)\big)\big]\big\}\end{aligned} \tag{24}$$

where $k = 2\pi/\lambda$ and λ is the wavelength.

By (23), we also have

$$\begin{aligned}\mathbf{H} = {} & n_0\big(-E_y\cos(\theta_0), -E_p, E_y\sin(\theta_0)\big) \\ & \times \exp\big\{i\big[\omega t - k\big(x\sin(\theta_0) + z\cos(\theta_0)\big)\big]\big\}\end{aligned}$$

The incidence of light on the plane $z = L_1$ produces transmitted vectors $\mathbf{E}_T^1, \ldots, \mathbf{E}_T^{m-1}$ in the layers $1, \ldots, m-1$ and the corresponding magnetic vectors $\mathbf{H}_T^1, \ldots, \mathbf{H}_T^{m-1}$. Simultaneously, reflected waves are produced, represented by the electric vectors $\mathbf{E}_R^0, \ldots, \mathbf{E}_R^{m-2}$ in the layers $0, 1, \ldots, m-2$ and the corresponding magnetic vectors $\mathbf{H}_R^0, \ldots, \mathbf{H}_R^{m-2}$.

As in (24), for $\nu = 1, \ldots, m-1$, taking into account the velocity of light in layer ν and the attenuation factor, we can write

$$\begin{aligned}\mathbf{E}_T^\nu = {} & \big(-E_{T,p}^\nu\cos(\theta_\nu), E_{T,y}^\nu, E_{T,p}^\nu\sin(\theta_\nu)\big) \\ & \times \exp\left\{i\left[\omega t - k\frac{n_\nu}{n_0}\big(x\sin(\theta_\nu) + z\cos(\theta_\nu)\big)\right]\right\} \\ & \times \exp\left(-\frac{k\kappa_\nu z}{n_0\cos(\theta_\nu)}\right)\end{aligned} \tag{25}$$

So, by a relation similar to (23) in layer ν,

$$\begin{aligned}\mathbf{H}_T^\nu = {} & n_\nu\big(-E_{T,y}^\nu\cos(\theta_\nu), -E_{T,p}^\nu, E_{T,y}^\nu\sin(\theta_\nu)\big) \\ & \times \exp\left\{i\left[\omega t - k\frac{n_\nu}{n_0}\big(x\sin(\theta_\nu) + z\cos(\theta_\nu)\big)\right]\right\} \\ & \times \exp\left(-\frac{k\kappa_\nu z}{n_0\cos(\theta_\nu)}\right)\end{aligned} \tag{26}$$

Similarly, for the reflected fields, with $\nu = 0, 1, \ldots, m-2$, we have

$$\begin{aligned}\mathbf{E}_R^\nu = {} & \big(E_{R,p}^\nu\cos(\theta_\nu), E_{R,y}^\nu, E_{R,p}^\nu\sin(\theta_\nu)\big) \\ & \times \exp\left\{i\left[\omega t - k\frac{n_\nu}{n_0}\big(x\sin(\theta_\nu) - z\cos(\theta_\nu)\big)\right]\right\} \\ & \times \exp\left(\frac{k\kappa_\nu z}{n_0\cos(\theta_\nu)}\right)\end{aligned} \tag{27}$$

and

$$\begin{aligned}\mathbf{H}_R^\nu = {} & n_\nu\big(E_{R,y}^\nu\cos(\theta_\nu), -E_{R,p}^\nu, E_{R,y}^\nu\sin(\theta_\nu)\big) \\ & \times \exp\left\{i\left[\omega t - k\frac{n_\nu}{n_0}\big(x\sin(\theta_\nu) - z\cos(\theta_\nu)\big)\right]\right\} \\ & \times \exp\left(\frac{k\kappa_\nu z}{n_0\cos(\theta_\nu)}\right)\end{aligned} \tag{28}$$

From electromagnetic theory, we know that the tangential component of the electric and the magnetic fields must be continuous at the interfaces. This means that

(i) The x and y components of $\mathbf{E} + \mathbf{E}_R^0$ must coincide with the x and y components of $\mathbf{E}_T^1 + \mathbf{E}_R^1$ for $z = L_1$.
(ii) The x and y components of $\mathbf{H} + \mathbf{H}_R^0$ must coincide with the x and y components of $\mathbf{H}_T^1 + \mathbf{H}_R^1$ for $z = L_1$.
(iii) The x and y components of $\mathbf{E}_T^\nu + \mathbf{E}_R^\nu$ must coincide with the x and y components of $\mathbf{E}_T^{\nu+1} + \mathbf{E}_R^{\nu+1}$ for $z = L_\nu$ for $\nu = 1, \ldots, m-3$.
(iv) The x and y components of $\mathbf{H}_T^\nu + \mathbf{H}_R^\nu$ must coincide with the x and y components of $\mathbf{H}_T^{\nu+1} + \mathbf{H}_R^{\nu+1}$ for $z = L_\nu$ for $\nu = 1, \ldots, m-3$.
(v) The x and y components of $\mathbf{E}_T^{m-2} + \mathbf{E}_R^{m-2}$ must coincide with the x and y components of $\mathbf{E}_T^{m-1}$ for $z = L_{m-1}$.
(vi) The x and y components of $\mathbf{H}_T^{m-2} + \mathbf{H}_R^{m-2}$ must coincide with the x and y components of $\mathbf{H}_T^{m-1}$ for $z = L_{m-1}$.

Let us define, for $\nu = 0, 1, 2, \ldots, m-2$,

$$\beta_\nu = \exp\left(\frac{k\kappa_\nu L_\nu}{n_0 \cos(\theta_\nu)} + \frac{ikn_\nu L_\nu \cos(\theta_\nu)}{n_0}\right) \tag{29}$$

$$\gamma_\nu = \exp\left(\frac{k\kappa_{\nu-1} L_\nu}{n_0 \cos(\theta_{\nu-1})} + \frac{ikn_{\nu-1} L_\nu \cos(\theta_{\nu-1})}{n_{r_0}}\right) \tag{30}$$

Then, by (24)–(30), the condition (iii) takes the form

$$E_{T,p}^{\nu-1} \frac{\cos(\theta_{\nu-1})}{\gamma_\nu} - E_{R,p}^{\nu-1} \cos(\theta_{\nu-1})\gamma_\nu - E_{T,p}^{\nu} \frac{\cos(\theta_\nu)}{\beta_\nu} + E_{R,p}^{\nu} \cos(\theta_\nu)\beta_\nu = 0 \tag{31}$$

$$E_{T,y}^{\nu-1} \frac{1}{\gamma_\nu} + E_{R,y}^{\nu-1}\gamma_\nu - E_{T,y}^{\nu} \frac{1}{\beta_\nu} - E_{R,y}^{\nu}\beta_\nu = 0 \tag{32}$$

for $\nu = 1, \ldots, m-3$. Analogously, condition (iv) takes the form

$$E_{T,y}^{\nu-1} \frac{n_{\nu-1} \cos(\theta_{\nu-1})}{\gamma_\nu} - E_{R,y}^{\nu-1} n_{\nu-1} \cos(\theta_{\nu-1})\gamma_\nu - E_{T,y}^{\nu} \frac{n_\nu \cos(\theta_\nu)}{\beta_\nu} + E_{R,y}^{\nu} n_\nu \cos(\theta_\nu)\beta_\nu = 0 \tag{33}$$

$$E_{T,p}^{\nu-1} \frac{n_{\nu-1}}{\gamma_\nu} + E_{R,p}^{\nu-1} n_{\nu-1}\gamma_\nu - E_{T,p}^{\nu} \frac{n_\nu}{\beta_\nu} - E_{R,p}^{\nu} n_\nu \beta_\nu = 0 \tag{34}$$

Moreover, adopting the definition $\mathbf{E}_T^0 = \mathbf{E}$ and writing $\mathbf{E}_R^{m-1} = \mathbf{0}$ (since there is no reflection in the last layer), we see that (31)–(34) also represent the continuity conditions (i), (ii), (v), and (vi). So, far, (31) and (34) form a system of $2(m-1)$ linear equations with $2(m-1)$ complex unknowns ($E_{T,p}^\nu$, $\nu = 1, \ldots, m-1$ and $E_{R,p}^\nu$, $\nu = 0, \ldots, m-2$). On the other hand, (32)–(33) form a similar system whose equations are $E_{T,y}^\nu$, $\nu = 1, \ldots, m-1$ and $E_{R,y}^\nu$, $\nu = 0, \ldots, m-2$. Both systems have a very special band-structure (each row of the matrix of coefficients has only four nonnull entries) and can be efficiently solved by Gaussian elimination. As a result, we can compute the transmitted energy and the reflected energy in the usual way:

$$\boxed{\textbf{Transmitted energy} = n_{m-1}\left|\mathbf{E}_T^{m-1}\right|^2}$$

and

$$\boxed{\textbf{Reflected energy} = n_0\left|\mathbf{E}_R^0\right|^2}$$

1.6. The Effect of a Thick Substrate

Assume that we have a stack of p films deposited on a thick substrate. By thick substrate we mean that the substrate thickness is much larger than the wavelength of light, whereas the film thicknesses are of the same order of magnitude as that wavelength. Consider first the case of an infinitely thick substrate. The transmittance is then defined in the substrate and reflections at the back substrate surface are neglected. Suppose, for example, that the incident medium is air ($n_0 = 1$) and one has an incident radiation of wavelength 995 nm. $n_1 = 2.1$ and $\kappa_1 = 0.1$ are the index of refraction and the extinction coefficient, respectively, of a unique $d = 127$-nm-thick film ($p = 1$) deposited onto a semi-infinite transparent substrate of refractive index $n_S = 1.57$. In this case, the transmittance is

$$T_{\text{semi-inf}} = 0.673819 \tag{35}$$

The above optical configuration is not realistic because, in general, the substrate supporting the films has a finite thickness. Reflections at the back surface of the transparent substrate will occur and the transmittance is now measured in an additional layer (usually air) which, in turn, is considered to be semi-infinite. Assuming a substrate thickness of exactly 10^6 nm $= 1$ mm, and performing the corresponding four-layer calculation ($(p+3)$-layer in the general case), we obtain

$$T_{\text{thick}=10^6\text{ nm}} = 0.590441 \tag{36}$$

The difference between $T_{\text{semi-inf}}$ and $T_{\text{thick}=10^6}$ is significant. Performing the same calculations with a substrate of thickness $10^6 + 150$ nm, we get

$$T_{\text{thick}=(10^6+150)\text{ nm}} = 0.664837 \tag{37}$$

Again, an important difference appears between $T_{\text{thick}=10^6\text{ nm}}$ and $T_{\text{thick}=(10^6+150)\text{ nm}}$. Note that, in practice, the two substrates are indistinguishable, their respective thicknesses differing by only 0.15 μm. This leads to the question of what we actually measure when we perform such experiments in the laboratory. Remember that the transmittance is a periodic function of the substrate thickness with a period of one-half wavelength. So, assuming random substrate thickness variations ($d_S \approx d_S \pm \Delta d_S$), with $\Delta d_S \approx \lambda_s/2$, we are led to conjecture that the measured transmission is better approximated by an average of transmissions over the period. This involves the integration of the transmittance as a function of the substrate thickness. In the above-mentioned example, this operation gives

$$T_{\text{average}} = 0.646609 \tag{38}$$

We arrive at the same value when we consider other indeterminations or perturbations to "exact" situations which normally happen in experimental setups, for example, slight deviations from normal incidence, or the fact that the measured wave (λ) is not a "pure" wave but contains wavelengths between $\lambda - \Delta\lambda$ and $\lambda + \Delta\lambda$, where $\Delta\lambda$ depends on the physical configuration of the measuring apparatus. It is worth mentioning that this $\pm\Delta\lambda$ "slit effect" alone does not explain the behavior of the transmission in real experiments. Slit widths commonly used in spectrophotometers are not large enough to eliminate completely interference effects that appear when one consider pure waves.

Fortunately, the integral leading to T_{average} in the general case can be solved analytically. The analytical integral has been done in [17]. The final formula is simple and admits a nice interpretation, which we give below. (See [17].)

Assume that the refractive index of the (transparent) substrate is n_S and the refractive index of the (transparent) final layer is n_F. By the arguments of previous sections on the two-layers case, when a wave defined in the substrate arrives at the back surface, it is refracted to the last layer with its energy multiplied by

$$\mathcal{T} = \frac{n_F}{n_S}\left[\frac{2n_S}{n_S + n_F}\right]^2 \tag{39}$$

and is reflected with its energy multiplied by

$$\mathcal{R} = \left[\frac{n_S - n_F}{n_S + n_F}\right]^2 \tag{40}$$

Consider, for a moment, that the substrate is semi-infinite and define

$T =$ transmittance from layer n_0 to the semi-infinite layer n_S of a wave with length λ;
$\overline{T} =$ transmittance from layer n_S to layer n_0 of a wave with length $\lambda(n_0/n_S)$;
$\overline{R} =$ reflectance in the same situation considered for $\overline{T}$ ($\overline{T} + \overline{R} \leq 1$).

In the above example, we have $\overline{T} = 0.673819$ and $\overline{R} = 0.186631$.

Assume a unit energy incident wave. Reasoning in energy terms (that is, not taking into account phase changes), we detect the total transmitted energy as the sum of infinitely many "small energies," as follows.

The first "small energy" comes from transmission through the films (T) followed by transmission through the substrate ($\mathcal{T}$), so it is equal to $T\,\mathcal{T}$.

The second "small energy" comes from transmission through the films (T), followed by reflection at the back-substrate ($\mathcal{R}$), followed by reflection at the back surface of the stack of films ($\overline{R}$), followed by transmission through the substrate ($\mathcal{T}$). Therefore, this "small energy" is equal to $R\,\mathcal{R}\,\overline{R}\,\mathcal{T}$.

The νth "small energy" comes from transmission through the films (T), followed by [reflection at the back-substrate ($\mathcal{R}$) and reflection at the back surface of the stack of films ($\overline{R}$)] $\nu - 1$ times, followed by transmission through the substrate ($\mathcal{T}$). Therefore, this "small energy" is equal to $T\,[\mathcal{R}\,\overline{R}]^{\nu-1}\,\mathcal{T}$.

Summing all the "small energies," we obtain

$$\text{Average transmittance} = \frac{T\mathcal{T}}{1 - \mathcal{R}\overline{R}}$$

Analogously, it can be obtained that

$$\text{Average reflectance} = \frac{T\overline{T}\mathcal{R}}{1 - \mathcal{R}\overline{R}}$$

The proof that these formulae correspond to the average integration of the transmittance and reflectance along the period can be found in [17].

1.6.1. Substrate on Top or Between Thin Films

Suppose now that a stack of thin films is covered by a thick transparent material. All the considerations above can be repeated, and the formulae for average transmittance and average reflectance turn out to be

$$\text{Average transmittance} = \frac{T\mathcal{T}}{1 - \mathcal{R}\overline{R}}$$

and

$$\text{Average reflectance} = R + \frac{T^2\mathcal{R}}{1 - \mathcal{R}\overline{R}}$$

where now

$$T = \frac{4n_0n_S}{(n_0 + n_S)^2} \quad \text{and} \quad R = \left(\frac{n_0 - n_S}{n_0 + n_S}\right)^2$$

$\mathcal{T}$ is the transmittance from the layer n_S (first layer now) to the last semi-infinite layer of a wave of length $\lambda n_0/n$, and $\mathcal{R}$ is the corresponding reflectance.

In some applications, a transparent thick substrate is covered with stacks of films on both sides with the purpose of getting some desired optical properties. As before, since the thickness of the substrate is much larger than the wavelength and, thus, than the period of transmittance and reflectance as functions of this thickness, a reasonable model for the measured transmittance and reflectance considers integrating these functions with respect to the period of the substrate. As shown in previous sections, if n_S and d_S are the refractive index and the thickness of the substrate, respectively, the period of the transmittance and of the reflectance as a function of d_S is $\lambda n_0/(2n_S)$, for an incident wave of length λ. At first sight, it is hard to integrate analytically T and R over the period. However, reasoning in energy terms, as done in a previous subsection, leads to the desired result. Let us define:

$T_1 =$ transmittance at λ through the upper stack of films, from layer n_0 to layer n_S;
$R_1 =$ reflectance of the previous situation;
$\overline{T}_1 =$ transmittance, for wavelength $\lambda n_0/n_S$, through the upper stack of films from layer n_S to layer n_0;
$\overline{R}_1 =$ reflectance corresponding to the $\overline{T}_1$ situation;

$T_2 =$ transmittance, for wavelength $\lambda n_0/n_S$, through the upper stack of films, from layer n_0 to layer n_S;
$R_2 =$ reflectance of the $\overline{T}_2$ situation.

Then, we get

$$\text{Transmittance from top stack to the substrate} = \frac{T_1 T_2}{1 - R_2 \overline{R}_1}$$

and

$$\text{Reflectance from top stack to the substrate} = R_1 + \frac{T_1 \overline{T}_1 R_2}{1 - R_2 \overline{R}_1}$$

This leads us to the previous case, a top substrate, with an effective transmittance and reflectance given by the above formulae.

1.7. Computational Filter Design

In this section, we consider that all the layers are transparent and, moreover, $n_0 = n_{m-1} = 1$. Therefore, the transmitted energy is $|t_{0,m-1}|^2$ and the reflected energy is $|r_{0,m-1}|^2$. For given wavelength λ and refraction coefficients $n_1, \ldots, n_{m-2}$, these energies are periodic functions of $d_1, \ldots, d_{m-2}$, the thicknesses of the intermediate layers. For some applications (lens design), it is necessary to determine the thicknesses of these layers in such a way that some objectives in terms of transmission and reflection are fulfilled [18]. For example, suppose that we want to design a system by the alternated superposition of four films of two different materials with refraction indices $n_L = 1.8$ and $n_H = 3.4$, in such a way that the transmission for a wavelength of 1000 nm is maximized, whereas the transmission for wavelengths λ such that $|\lambda - 1000| \leq 10$ is minimal. We can do this solving the following optimization problem:

$$\text{Maximize } f(d_1, \ldots, d_{m-2}) \tag{41}$$

where

$$\begin{aligned} &f(d_1, \ldots, d_{m-2}) \\ &\quad = \left|t_{5,0}\big(\lambda = 1000, (d_1, \ldots, d_{m-2})\big)\right|^2 \\ &\qquad - \text{Average}_{|\lambda-1000|\geq 10}\left|t_{6,1}\big(\lambda, (d_1, \ldots, d_{m-2})\big)\right|^2 \end{aligned}$$

Note that, although the function $|t_{5,0}|^2$ is periodic with respect to each thickness, this is not the case of f. As a result, f has many local maximizers that are not true solutions of (41).

The gradient of f can be computed recursively using the scheme presented in the previous section, so that a first-order algorithm for optimization can be used to solve the problem. We used the algorithm [19] (see also [20]) for solving the problem, with 500 nm as an initial estimate of all the thicknesses. For these thicknesses, the transmission for $\lambda = 1000$ is 0.181 and the average of the "side-transmissions" is 0.515. The algorithm has no difficulties in finding a (perhaps local) minimizer using eight iterations and less than five seconds of computer time in a Sun workstation. The resulting transmission for $\lambda = 1000$ is 0.9999, whereas the average of the side-transmissions is 0.358. The thicknesses found are 556.3, 508.7, 565.6, and 509.9 nm, respectively.

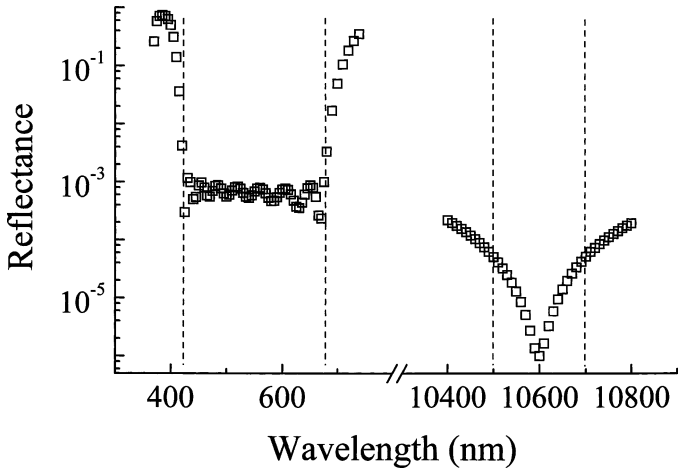

Fig. 8. Reflectance in the visible and infrared spectral regions of the optimized dual-band antireflection coating.

Dual-band antireflection filter. Consider, as a final example, the following design problem. Given air as the incident medium, a nonabsorbing sibstrate (sub), and two nonabsorbing coating materials (L and H), produce an antireflection that reduces simultaneously the reflectance to the lowest possible values in two spectral regions: (1) 420 nm to 680 nm; and (2) 10500 nm to 10700 nm.

The foregoing requirements are to be for dielectric and substrate layers having the following index of refraction:

$$\begin{aligned} n_{\text{sub}}(1) &= 2.60 \qquad n_{\text{sub}}(2) = 2.40 \\ n_L(1) &= 1.52 \qquad n_L(2) = 1.43 \\ n_H(1) &= 2.32 \qquad n_H(2) = 2.22 \end{aligned}$$

There is restriction neither to the thickness of the individual layers nor to the number of layers. The dual-band problem has been solved as an optimization problem. The objective function was the sum of the reflectances in the two bands. This function was minimized with respect to the thicknesses using the algorithm described in [19]. This algorithm can be freely obtained in [20]. The minimization was performed in several steps, increasing the number of films that are present in the stack. Given the solution for a number of films, an additional film was added with zero thickness, in an optimal position determined by the needle technique [21]. According to this technique, the position of the new zero-thickness film is the best possible one in the sense that the partial derivative that corresponds to its position is negative and minimal. In other words, the potentiality of decreasing locally the objective function for the needle-position of the zero-film is maximized.

Figure 8 shows the results of the optimization process for a total of 20 layers. The total thickness of the stack is 1560 nm. Note that the maximum reflection in the two bands is approximately 0.1%, the reflectance being smaller in the infrared than in the visible spectral region. It is clear that this is not the only solution to the problem [22]. In principle, an increasing number of layers should improve the performance of the dual-band antireflection filter. The manufacturing of filters always entails

small random variations of the individual layer thickness. When a random thickness variation of, say, 1% is applied to the stack, a tenfold increase of the mean reflectance is normally found. The effect becomes more severe as the number of layers increases.

1.8. Optimization Algorithm for Thin Films

The method used for solving the optimization problems derived from thin-film calculations is a trust-region box-constraint optimization software developed at the Applied Mathematics Department of the State University of Campinas. During the last five years, it has been used for solving many practical and academic problems with box constraints, and it has been incorporated as a subalgorithm of Augmented Lagrangian methods for minimization with equality constraints and bounds. This software is called BOX-QUACAN here. Its current version is publicly available as the code EASY! in `www.ime.unicamp.br/~martinez`. The problems solved in the present context are of the type

$$\text{Minimize } f(x)$$

subject to $x \in \Omega \subset \mathbb{R}^n$. Ω is a set defined by simple constraints. In our case, the thicknesses must be nonnegative or restricted to some lower bounds. The art of minimization with simple constraints is known as box-constrained optimization. Actually, this is a well-developed area of numerical analysis.

BOX-QUACAN is a box-constraint solver whose basic principles are described in [19]. It is an iterative method which, at each iteration, approximates the objective function by a quadratic and minimizes this quadratic model in the box determined by the natural constraints and an auxiliary box that represents the region where the quadratic approximation is reliable (trust region). If the objective function is sufficiently reduced at the (approximate) minimizer of the quadratic, the corresponding trial point is accepted as the new iterate. Otherwise, the trust region is reduced. The subroutine that minimizes the quadratic is called QUACAN and the main algorithm, which handles trust-region modifications, is BOX.

Assume that Ω is an n-dimensional box, given by

$$\Omega = \{x \in \mathbb{R}^n \mid \ell \le x \le u\}$$

So, the problem consists of finding an approximate solution of

$$\text{Minimize}_x \ f(x) \quad \text{subject to } \ell \le x \le u \tag{42}$$

BOX-QUACAN uses sequential (approximate) minimization of second-order quadratic approximations with simple bounds. The bounds for the quadratic model come from the intersection of the original box with a trust region defined by the ∞-norm. No factorization of matrices are used at any stage. The quadratic solver used to deal with the subproblems of the box-constrained algorithm visits the different faces of its domain using conjugate gradients on the interior of each face and "chopped gradients" as search directions to leave the faces. See [19, 23, 24] for a description of the 1998 implementation of QUACAN. At each iteration of this quadratic solver, a matrix-vector product of the Hessian approximation and a vector is needed. Since Hessian approximations are cumbersome to compute, we use the "Truncated Newton" approach, so that each *Hessian* $\times$ *vector* product is replaced by an incremental quotient of ∇f along the direction given by the vector.

The box-constraint solver BOX is a trust-region method whose convergence results have been given in [19]. Roughly speaking, if the objective function has continuous partial derivatives and the Hessian approximations are bounded, every limit point of a sequence generated by BOX is stationary. When one uses true Hessians or secant approximations (see [25]) and the quadratic subproblems are solved with increasing accuracy, quadratic or superlinear convergence can be expected. In our implementation, we used a fixed tolerance as stopping criterion for the quadratic solver QUACAN, because the benefits of high-order convergence of BOX would not compensate increasing the work of the quadratic solver. It is interesting to note that, although one usually talks about "Hessian approximations," second derivatives of the objective function are not assumed to exist at all. Moreover, global convergence results hold even without the Hessian-existence assumption.

2. APPLICATIONS OF THIN FILMS

In this section, we discuss a few situations where the theoretical considerations of the previous section are put to work. The subject of thin-film applications is very vast and impossible to be detailed in a book chapter. The selection to follow considers, as usual, the most classical structures and those with which the authors have been particularly involved. For a discussion of remaining subjects we refer the readers to the specialized literature [8, 9, 16, 18, 27–30].

2.1. Antireflection Coatings

The reflectance between two different (thick) dielectric materials for a light beam falling normally to the interface is given approximately by $R = (n_1 - n_2)^2/(n_1 + n_2)^2$ and it may be quite important in dense materials. In an air/glass interface, around 4% of the incident light is reflected. Hence, for a normal lens, the loss amounts to $\approx$8%. For an optical system including a large number of lenses, the optical performance may be severely affected. For a silicon solar cell ($n_{\text{Si}} \approx 4$), the optical losses, of the order of 35%, reduce considerably the conversion efficiency.

The amount of reflected light may be diminished significantly by depositing thin intermediate antireflection (AR) layers. The subject is addressed in most textbooks on elementary optics as well as in the specialized literature on the physics of thin films. An exact theoretical derivation of reflection-reducing optical coatings from Maxwell equations and boundary conditions between layer and substrate has been given by Mooney [31]. The analysis considers normal incidence

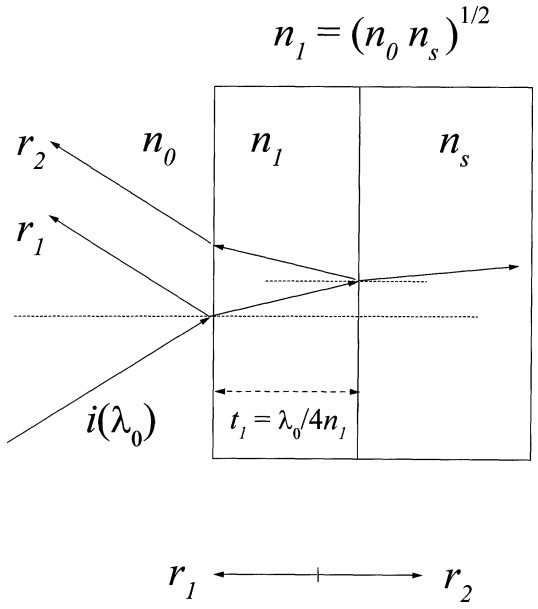

Fig. 9. Single antireflection layer onto a thick substrate. The figure shows the conditions of zero reflectance at wavelength λ_0.

and isotropic flat parallel dielectric materials. The analytical expressions for the reflectivity, defined as the ratio of the intensity of the reflected beam to that of the incident beam, is

$$\begin{aligned} R = {} & \Big\{\big[(\varepsilon_1)^{1/2} + (\varepsilon_S)^{1/2}\big]^2\big[1 - (\varepsilon_1)^{1/2}\big]^2 \\ & + \big[(\varepsilon_1)^{1/2} - (\varepsilon_S)^{1/2}\big]^2\big[1 + (\varepsilon_1)^{1/2}\big]^2 \\ & + 2(\varepsilon_1 - \varepsilon_S)(1 - \varepsilon_1)\cos(2k_1 t)\Big\} \\ & \times \Big\{\big[(\varepsilon_1)^{1/2} + (\varepsilon_S)^{1/2}\big]^2\big[1 + (\varepsilon_1)^{1/2}\big]^2 \\ & \quad + \big[(\varepsilon_1)^{1/2} - (\varepsilon_S)^{1/2}\big]^2\big[1 - (\varepsilon_1)^{1/2}\big]^2 \\ & \quad + 2(\varepsilon_1 - \varepsilon_S)(1 - \varepsilon_1)\cos(2k_1 t)\Big\}^{-1} \end{aligned}$$

where medium 0 is air, medium 1 is the optical coating, and S is the substrate. The minimum R occurs for $t = \pi/2k_1 = \lambda_0/4\sqrt{\varepsilon_1}$ and for all odd integral multiples of this thickness. Under these circumstances, the beams reflected at the air/layer and at the layer/substrate interfaces interfere destructively, as shown in Figure 9. The minimum reflectance reads

$$R_{\min}(\lambda_1) = \left[\frac{(\varepsilon_S)^{1/2} - \varepsilon_1}{(\varepsilon_S)^{1/2} + \varepsilon_1}\right]^2$$

The condition for zero reflection of a single coating can be obtained at a wavelength λ_0 if $\varepsilon_1(\lambda_0) = \sqrt{\varepsilon_s(\lambda_0)}$, or $n_1 = \sqrt{n_s}$ if the material is transparent at λ_0. The relation guarantees that the intensity reflected at each of the two interfaces is the same. If air is not the medium where the light beam comes from ($\varepsilon_0 > 1$), the condition for zero reflection for odd multiples of a quarter-wavelength thickness becomes $\varepsilon_1 = (\varepsilon_0\varepsilon_s)^{1/2}$. For the case of a typical glass $n_G \approx 1.5$/air interface, the antireflection layer should possess an index $n_1 = 1.225$ for a perfect match. Stable materials having this low index value do not exist. Instead, MgF_2 ($n \approx 1.38$) can be used, allowing a larger than 2% reduction of the reflectance. Table I lists the refractive indices of some materials.

Table I. Refractive Indices of Some Materials

Material	Index	Material	Index
MgF_2	1.3–1.4	Si_3N_4	1.9–1.95
SiO_2	1.4–1.5	TiO_2	2.3–2.4
Al_2O_3	1.7–1.8	Ta_2O_5	2.1–2.3
SiO	1.8–1.9	ZnS	2.5
SnO_2	1.8–1.9	Diamond	2.4

Note that the values given in Table I correspond to refractive indices measured in the transparent regions of the spectrum, in other words, far from the absorption edge, where the index of refraction increases with photon energy. Variations of the refractive index with photon energy can be included in the design of antireflection coatings. The calculations, however, become more involved and numerical methods are required.

A double-layer coating using two different dielectrics, 1 and 2, allows zero reflectance at two different wavelengths. The condition for an equal intensity of reflection at each of the three interfaces is now expressed as $n_0/n_1 = n_1/n_2 = n_2/n_s$. Quarter-wavelength-thick layers of such materials, $\lambda_0/4n_1$ and $\lambda_0/4n_2$, produce destructive interference at wavelengths $3/4\lambda_0$ and $3/2\lambda_0$, at which the phase difference Θ between the beams reflected at the three interfaces equals 120° and 240°, respectively, as shown in Figure 10. The theory can be extended to a larger number of layers giving an achromatic antireflection coating. Three appropriate AR layers offers the possibility of zero reflectance at three different wavelengths, etc. As the number of layers increases, however, the benefits may not compensate the additional technical difficulties associated with the deposition of extra films.

The refractive index match of a large number of layers needed to obtain zero reflection may become difficult to meet. However, as the resulting reflectance is approximately given by the vector sum of the Fresnel coefficients at the interfaces, a zero reflectance at a given wavelength can be met using the film thickness as a design variable. The required condition is that the Fresnel coefficients $r_1, \ldots, r_n$ form a closed polygon at the selected wavelength [17].

The same kind of analysis may be applied to the circumstance where a high reflectance is desired at a particular wavelength. Besides metals, dielectric and semiconductor materials can be used for this purpose. Quarter-wavelength layers are still used, but the refractive index of the coating should be greater than that of the substrate; in fact, the difference should be as large as possible. ZnS, TiO_2, and Ta_2O_5 are used onto glass for applications in the visible spectrum. For infrared radiation, a collection of very dense materials exists, such as Si ($n \sim 3.5$), Ge ($n \sim 4$), and the lead salts (PbS, PbSe, and PbTe), to cite a few. With these materials, it is possible to have reflected intensities larger than 80%.

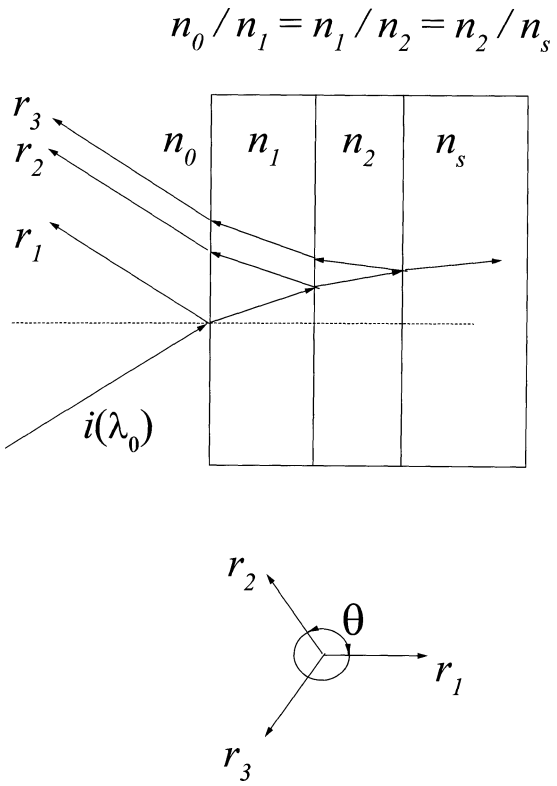

Fig. 10. Quarter-wavelength double antireflection coating. The figure illustrates the conditions for index match to produce zero reflectance at wavelengths $3/4\lambda_0$ and $3/2\lambda_0$.

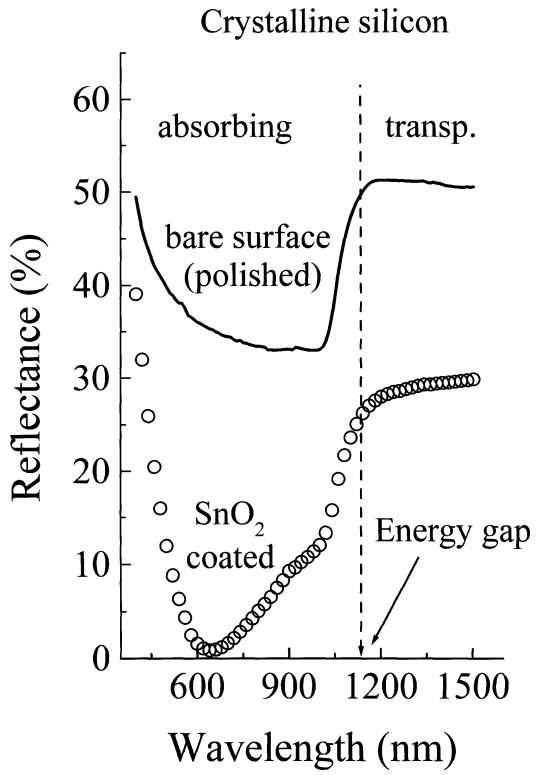

Fig. 11. Reflectance (%) of a polished crystalline silicon wafer as a function of wavelength. The open circles indicate the reflectance measured after spraying a 77-nm-thick SnO_2 layer.

Multiple-layer reflector structures employ an odd large number of stacked dielectric films of quarter-wavelength thickness. The stacking alternates layers of a large and a small index of refraction. The reflected rays of all the interfaces of the structure emerge in phase for the selected wavelength, at which a reflectance of nearly 100% can be obtained. The high reflectance, however, exists for a rather narrow frequency range because the phase change at the interfaces depends on wavelength. The expressions giving the reflectance and the transmittance of such structures as a function of wavelength are rather lengthy but can be optimized without difficulty using the formulation given in the previous section.

2.1.1. Antireflection Coatings for Solar Cells

Solar cells are devices that directly convert sunlight into electricity. We will not review here the basic mechanisms of solar electricity generation, but simply note that antireflection coatings are of utmost importance to improve the conversion efficiency of the device. As a consequence, the subject has received much attention in the last decades, when solar electricity generation became an interesting alternative for many terrestrial applications. Silicon, either single-crystal or polycrystalline, is the base semiconductor material dominating the industrial manufacturing of solar cells. Other semiconductor alloys, such as hydrogenated amorphous silicon (a-Si:H), CdTe, and $CuInSe_2$, are emerging materials for photovoltaic applications. Let us consider the reflectance of a single-crystal silicon solar cell. Figure 11 illustrates the situation. The continuous line is the measured reflectance of a polished, 400-μm-thick, Si wafer ($n_{\rm Si} \geq 3.4$). The vertical dashed line roughly indicates the boundary between complete absorption and transparency. In the transparent region, the reflectance is high due to the large index of silicon and to the contribution of the two faces of the wafer to the overall reflectance. For wavelengths smaller than $\sim$1130 nm, the reflectance decreases because of light absorption in the wafer, which diminishes the contribution of the reflection at the back Si–air interface. At $\lambda \lesssim 1050$ nm, the back interface does not contribute any more and the measured reflectance corresponds to the front interface only. The increased reflectance at $\lambda \lesssim 1050$ nm derives from an increasing $n_{\rm Si}$. The open symbols indicate the reflectance measured of the same Si wafer after spraying an SnO_2 AR coating. The situation depicted in Figure 11 deserves some additional comments.

(a) First, in order to work as an electric generator, photons must be absorbed in the silicon substrate; that is, the photons of interest possess an energy larger than the Si band-gap [$\hbar\omega > E_g(\mathrm{Si}) \approx 1.1$ eV, or $\lambda < \lambda_{\rm gap} \approx 1130$ nm].

(b) Second, the solar spectrum is very broad [32]. The continuous line in Figure 12 shows the irradiance of sunlight, or its spectral intensity distribution, in the wavelength range of interest for the present discussion. Note the radiance units on the left ordinate. The area below the complete curve gives

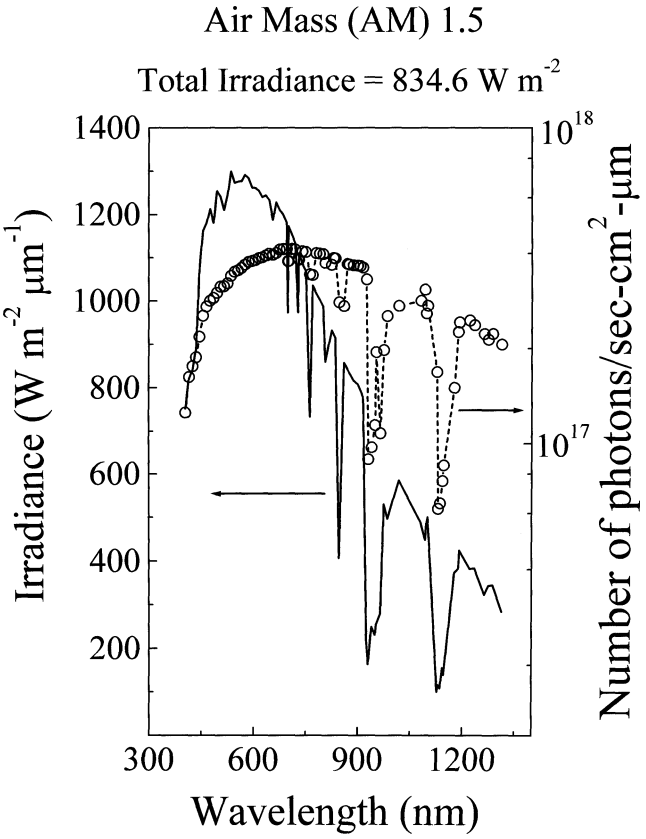

Fig. 12. Air Mass 1.5 solar spectrum. Full line: irradiance (power density) per unit wavelength interval. Open circles: photon flux density per unit energy interval. Note that for solar cells (quantum detectors), it is the reflected photon flux that has to be minimized, not the irradiance.

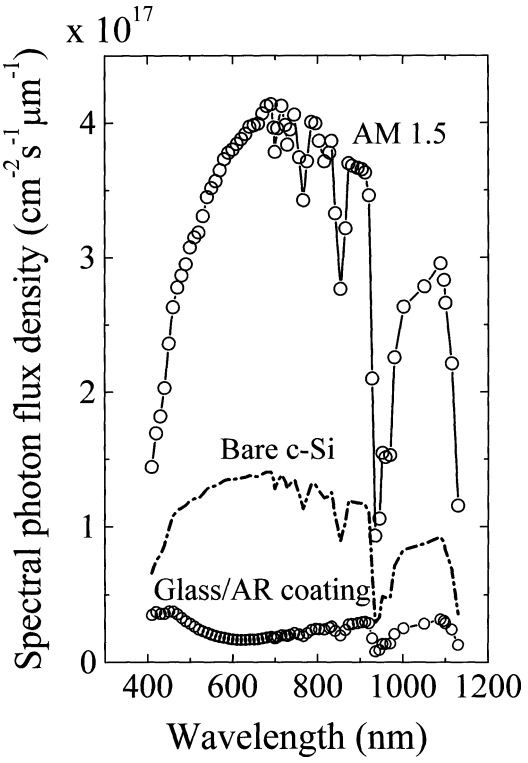

Fig. 13. Spectral photon flux density under AM 1.5 irradiation conditions. The dotted-dashed curve indicates the photon flux density reflected by a polished silicon surface (solar cell). The open circles at the bottom of the figure show the photon reflection in a system consisting of a cover glass, an optimized AR coating, and a crystalline silicon solar cell. The optimization finds the index of refraction and the thickness of the AR coating that minimizes the sum of reflected useful photons of the AM 1.5 solar spectrum. See text.

834.6 $W \cdot m^{-2}$, and this value corresponds to a clear day with the sun inclined 48° (AM 1.5) with respect to the normal [32]. The spectrum shows several absorption bands originating mainly from water vapor and carbon oxides.

(c) Third, absorbed photons means working in a photon energy region where the optical constants of the substrate silicon strongly depend on wavelength.

(d) Fourth, solar cells are quantum detectors; that is, electrons are excited through photon absorption. In other words, in order to maximize the photocurrent of the solar cell, the total amount of reflected photons has to be minimized in the energy range of interest, and not the reflectance (intensity). Remember that photon energy is inversely proportional to wavelength. The open circles in Figure 12 show the photon density per unit wavelength interval versus wavelength for the same radiance spectrum given by the continuous line. The area below this curve for energies smaller than the energy gap gives the total number of absorbed photons. This is the spectrum to be considered for photovoltaic AR coatings.

(e) Fifth, the optimization of the photocurrent in a solar cell must also consider: (1) the internal collection efficiency, which measures the amount of collected electrons at the electrical contacts per absorbed photon, and (2) the variations of the refractive index with wavelength. In a good device, the collection efficiency $\eta \simeq 1$ for most absorbed photons. In general, it decreases at short wavelengths due to surface effects. At long wavelengths, photon absorption decreases because of a decrease of the absorption coefficient, and the photocurrent drops.

Summarizing, the optimization of an antireflection coating on a solar cell should include the variations of the refractive index of the substrate material in the range of high absorption and the quantum nature of the conversion process (photon spectral distribution of the solar spectrum).

As an illustrative case, we present below the results of minimizing the reflected photon flux in a solar converter system consisting of a 4-mm protecting glass ($n = 1.52$), an AR coating (to be optimized), and a crystalline silicon solar cell. The input data are the index of refraction of the glass cover, the optical properties of crystalline silicon, and the photon flux density of the AM 1.5 solar spectrum (see Fig. 12). We consider normal incidence for the photon flux and the 400- to 1130-nm photon wavelength range. The minimization algorithm finds $n = 2.41$ and $d = 66$ nm for the AR coating that will maximize the energy output of the system. The results on reflectance are shown in Figure 13.

The above optimization will just consider the photon distribution of a particular sunlight spectrum. In fact, the important

parameter to be maximized is the electric energy delivered by the device. In other words, a complete optimization should consider the position of the sun in the sky along the day and along the year (angle of incidence), as well as the variations of the solar spectrum with prevailing weather conditions.

2.2. A Reverse Engineering Problem: The Retrieval of the Optical Constants and the Thickness of Thin Films from Transmission Data

Thin-film electronics includes thin-film transistors and amorphous semiconductor solar cells. In many circumstances, the thickness d and the optical properties $n(\lambda) - i\kappa(\lambda)$ must be known with some degree of accuracy. As shown in a previous section, measurements of the complex amplitudes of the light transmitted and reflected at normal or oblique incidence at the film and substrate sides, or different combinations of them, enable the explicit evaluation of the thickness and the optical constants in a broad spectral range. For electronic applications, however, the interesting photon energy range covers the neighborhood of the fundamental absorption edge in which the material goes from complete opacity to some degree of transparency. As optical transmittance provides accurate and quick information in this spectral range, efforts have been made to develop methods allowing the retrieval of the thickness and the optical constants of thin films from transmittance data only.

Figure 14 shows three transmission spectra typical of thin isotropic and homogeneous dielectric films, bounded by plane-parallel surfaces and deposited onto transparent thick substrates. They correspond to: (a) a film, thick enough to display interference fringes coming from multiple coherent reflections at the interfaces and being highly transparent below the fundamental absorption edge; (b) a thick film, as above, but strongly absorbing in all the measured spectral range; and (c) a very thin film not showing any fringe pattern in the spectral region of interest. The interference fringes of films having a transparent spectral region, such as the ones shown by film 14a, can be used to estimate the film thickness and the real part of the index of refraction in this region [8, 33–35]. The approach is known as the envelope method, first proposed by Manifacier et al. [34]. The calculation of the optical constants in the absorbing region, however, cannot be estimated in a simple way. Usually, a functional dependence for $n(\lambda)$ is assumed, in most cases a function of the type $n = A\lambda^{-2} + B\lambda + C$ (where A, B, and C are constants), to extrapolate the index values estimated in the transparent region of the spectrum to higher photon energies [35]. Knowing d and $n(\lambda)$, the absorption coefficient can be calculated from the general expression of the transmission. In general, these approximations are of limited accuracy and result in a poor estimate of the absorption coefficient. Moreover, films not possessing a transparent spectral region (see film 14b), or too thin to display optical fringes in the measured range (see film 14c), cannot be solved by these approximate methods, which use transmission data only.

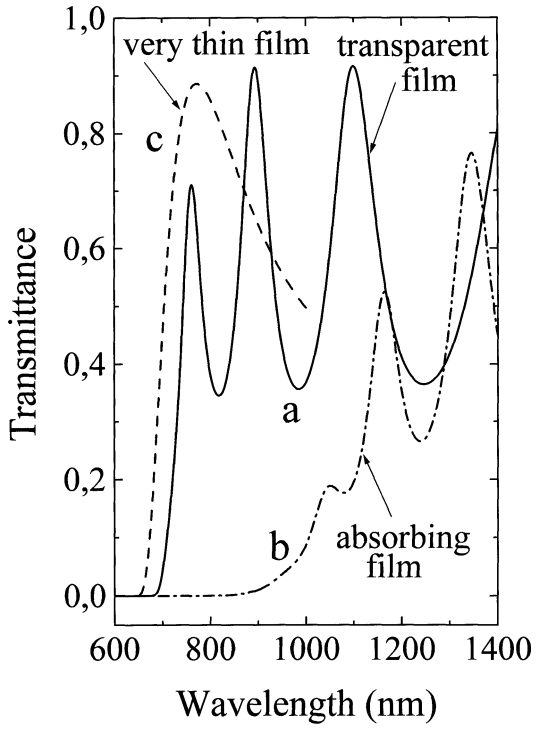

Fig. 14. Transmittance in the 600- to 1400-nm wavelength of three typical semiconductor thin films. Spectrum *a* corresponds to a relatively thick film displaying a fringe pattern in a region of very weak absorption. Spectrum *b* sketches the transmittance of a thick absorbing semiconductor film. There is no useful fringe pattern in the measured wavelength range. Spectrum *c* illustrates the transmittance of a rather thin film not displaying a fringe pattern.

Before discussing new retrieval algorithms, let us first consider in some detail the optical transmission measurements through thick transparent substrates (or layers).

2.2.1. Measured Transmission and the Four-Layer Case

In real cases, what is measured is not the transmittance of pure waves with a single λ. The detectors always indicate a signal corresponding to a wave packet of a finite bandwidth ($\pm\Delta\lambda$) centered around λ. Hence, the measured transmittance data of an *air/film/thick substrate/air* system ($n_0/n_1/n_S/n_0$) represent an average transmittance, or a signal integrated in a very narrow frequency band, the width of which depends on a chosen slit or other experimental conditions. Therefore, what is measured is not $|t_{m-1,0}(\lambda)|^2$ but:

$$\text{Measured transmission} = \frac{1}{2\Delta\lambda}\int_{\lambda-\Delta\lambda}^{\lambda+\Delta\lambda} \left|t_{m-1,0}(\lambda)\right|^2 d\lambda$$

where $\pm\Delta\lambda$ corresponds to the mentioned experimental bandpass centered around λ.

As mentioned in a previous section, $|t_{m-1,0}(\lambda)|^2$ is a periodic function of film thickness, with period $\lambda/(2n_1)$. Usually, the length of this period is smaller than the substrate thickness, say $[\lambda/(2n_1)]/d_S \sim 10^{-3}$–$10^{-4}$. Such values are, in turn, of the order of, or smaller than, the error associated to the measured substrate thickness. As a consequence, a reasonable approxima-

tion to the measured transmittance is an average over the entire period:

$$\text{Measured transmission (2)} = \frac{2n_1}{\lambda}\int_{d_S}^{d_S+\lambda/(2n_1)} \left|t_{m,1}(\lambda, d_S)\right|^2 d(d_S) \tag{43}$$

The integral (43) can be calculated analytically and, clearly, does not depend on the substrate thickness d_S. The discussion can be easily extended to the multilayer case.

Assume now, as above, that we are in the mentioned four-layer situation: *air* (n_0)/*film* (n_1)/*thick substrate* (n_S)/*air* (n_0). For the sake of simplicity of notation, let us call, from now on, d, n, and κ the thickness, the refractive index, and the attenuation coefficient of the film, and s the refractive index of the substrate. In this case, (43) reduces to

$$T = \text{Measured transmission (2)} = \frac{Ax}{B - Cx + Dx^2} \tag{44}$$

where

$$A = 16s\left(n^2 + \kappa^2\right) \tag{45}$$

$$B = \left[(n+1)^2 + \kappa^2\right]\left[(n+1)\left(n + s^2\right) + \kappa^2\right] \tag{46}$$

$$C = \left[\left(n^2 - 1 + \kappa^2\right)\left(n^2 - s^2 + \kappa^2\right) - 2\kappa^2\left(s^2 + 1\right)\right]2\cos\varphi - \kappa\left[2\left(n^2 - s^2 + \kappa^2\right) + \left(s^2 + 1\right)\left(n^2 - 1 + \kappa^2\right)\right]2\sin\varphi \tag{47}$$

$$D = \left[(n-1)^2 + \kappa^2\right]\left[(n-1)\left(n - s^2\right) + \kappa^2\right] \tag{48}$$

$$\varphi = 4\pi nd/\lambda \qquad x = \exp(-\alpha d) \qquad \alpha = 4\pi\kappa/\lambda \tag{49}$$

2.2.2. *Pointwise Optimization Approach*

Consider now the problem of estimating the absorption coefficient, the refractive index, and the thickness of a thin film, as in the above example, using only transmittance data for (many) different wavelengths. The theoretical transmission is given by (44), where the refractive index of the substrate s is known and $n(\lambda)$, $\alpha(\lambda)$, and d are the unknowns. At first glance, this problem is highly underdetermined since, for each wavelength, the single equation

$$\boxed{\text{Theoretical transmission} = \text{Measured transmission}} \tag{50}$$

has three unknowns d, $n(\lambda)$, $\alpha(\lambda)$, and only d is repeated for all values of λ. One way to decrease the degrees of freedom of (50), at a point that only physically meaningful estimated parameters are admissible, is to consider a prior knowledge of the functions $n(\lambda)$, $\alpha(\lambda)$. The idea of assuming a closed formula for n and α depending on a few coefficients has been explored in envelope methods [33–35]. These methods are efficient when the transmission curve exhibits a fringe pattern, representing a rather large zone of the spectrum, where $\alpha(\lambda)$ is almost null. In other cases, the fulfillment of (50) can be very crude or the curves $n(\lambda)$, $\alpha(\lambda)$ are physically unacceptable.

In [36, 37], instead of imposing a functional form for $n(\lambda)$ and $\kappa(\lambda)$, the phenomenological constraints that restrict the variability of these functions were stated explicitly, so that the estimation problem takes the form:

$$\text{Minimize} \quad \sum_{\lambda}\big[\text{Theoretical transmission}(\lambda) - \text{Measured transmission}(\lambda)\big]^2$$
$$\text{subject to Physical Constraints} \tag{51}$$

In this way, well-behaved functions $n(\lambda)$ and $\kappa(\lambda)$ can be obtained without severe restrictions that could damage the quality of the fitting (50).

At this point, it is convenient to say that the main inconvenience of the pointwise constrained optimization approach [36, 37] is that (51) is a rather complex large-scale linearly constrained nonlinear programming problem whose solution can be obtained only by means of rather sophisticated and not always available computer codes that can deal effectively with the sparsity of the matrix of constraints. See [38, 39].

A second approach was established in [40] for solving the estimation problem. In the new method, (51) is replaced by an unconstrained optimization problem. We solved this problem using a very simple algorithm introduced recently by Raydan [41], which realizes a very effective idea for potentially large-scale unconstrained minimization. It consists of using only gradient directions with steplengths that ensure rapid convergence. The reduction of (51) to an unconstrained minimization problem needs the calculation of very complicated derivatives of functions, which requires the use of automatic differentiation techniques. The present authors used the procedures for automatic differentiation described in [42]. Before addressing the unconstrained optimization approach, let us consider the main ideas behind the pointwise optimization, as well as its effectiveness in retrieving the optical constants and the thickness of *gedanken* and real films.

A set of experimental transmittance data $(\lambda_i, T^{\text{meas}}(\lambda_i))$, $i = 1, \ldots, N$, $\lambda_{\min} \le \lambda_i < \lambda_{i+1} \le \lambda_{\max}$ for all $i = 1, \ldots, N$) is given, $s(\lambda)$ is known, and we want to estimate d, $n(\lambda)$, and $\alpha(\lambda)$. As said, the problem is highly underdetermined because, for a given d and any λ, the following equation must hold:

$$T^{\text{calc}}\big(\lambda, s(\lambda), d, n(\lambda), \kappa(\lambda)\big) = T^{\text{meas}}(\lambda)$$

Equation (44) has two unknowns $n(\lambda)$ and $\alpha(\lambda)$ and, therefore, its set of solutions is, in general, a curve in the two-dimensional $(n(\lambda), \alpha(\lambda))$ space. As a consequence, the set of functions (n, α) that satisfy (44) for a given d is infinite and, roughly speaking, is represented by a nonlinear manifold of dimension N in $\mathbb{R}^{2N}$.

However, physical constraints reduce drastically the range of variability of the unknowns $n(\lambda)$, $\alpha(\lambda)$. The type of constraints which relate n and α at different wavelengths derive from a prior knowledge of the physical solution. To illustrate the approach, let us consider, for example, the behavior of the optical constants of an amorphous (a-)semiconductor thin film deposited onto a thick glass substrate. In the neighborhood

of the fundamental absorption edge of a-semiconductors, it is known that:

PC1: $n(\lambda) \geq 1$, $\alpha(\lambda) \geq 0$ for all $\lambda \in [\lambda_{\min}, \lambda_{\max}]$;
PC2: $n(\lambda)$ and $\alpha(\lambda)$ are decreasing functions of λ;
PC3: $n(\lambda)$ is convex;
PC4: in a $\log(\alpha)$ vs. $\hbar\omega$ (photon energy) plot, the absorption coefficient α of an a-semiconductor has an elongated $\int$-like shape. Thus, for the spectral region corresponding to the exponential absorption edge, and smaller photon energies, there exists $\lambda_{\text{infl}} \in [\lambda_{\min}, \lambda_{\max}]$ such that $\alpha(\lambda)$ is convex if $\lambda \geq \lambda_{\text{infl}}$ and concave if $\lambda < \lambda_{\text{infl}}$.

The constraints **PC1**, **PC2**, **PC3**, and **PC4** relate unknowns of (50) for different indices i. So, (50) cannot be considered independent anymore and its degrees of freedom are restricted. From these considerations, the problem of determining d, n, and α in a selected spectral region can be modeled minimizing

$$\sum_{i=1}^{N}\left[T_i^{\text{calc}}\big(\lambda, s(\lambda), d, n(\lambda), \alpha(\lambda)\big) - T^{\text{meas}}(\lambda)\right]^2$$

subject to constraints **PC1**, **PC2**, **PC3**, and **PC4**. For obvious reasons, this is called a *pointwise constrained optimization approach* for the resolution of the estimation problem.

Observe that, assuming **PC2**, **PC1** is satisfied under the sole assumption $n(\lambda_{\max}) \geq 1$ and $\kappa(\lambda_{\max}) \geq 0$.

The constraints **PC2**, **PC3**, and **PC4** can be written, respectively, as

$$n'(\lambda) \leq 0 \qquad \kappa'(\lambda) \leq 0 \quad \text{for all } \lambda \in [\lambda_{\min}, \lambda_{\max}] \tag{52}$$

$$n''(\lambda) \geq 0 \quad \text{for all } \lambda \in [\lambda_{\min}, \lambda_{\max}] \tag{53}$$

$$\kappa''(\lambda) \geq 0 \quad \text{for } \lambda \in [\lambda_{\text{infl}}, \lambda_{\max}] \quad \text{and}$$

$$\kappa''(\lambda) \leq 0 \quad \text{for } \lambda \in [\lambda_{\min}, \lambda_{\text{infl}}] \tag{54}$$

Clearly, the constraints

$$n''(\lambda) \geq 0 \quad \text{for all } \lambda \in [\lambda_{\min}, \lambda_{\max}] \quad \text{and} \quad n'(\lambda_{\max}) \leq 0$$

imply that

$$n'(\lambda) \leq 0 \quad \text{for all } \lambda \in [\lambda_{\min}, \lambda_{\max}]$$

Moreover,

$$\kappa''(\lambda) \geq 0 \quad \text{for all } \lambda \in [\lambda_{\text{infl}}, \lambda_{\max}] \quad \text{and} \quad \kappa'(\lambda_{\max}) \leq 0$$

imply that

$$\kappa'(\lambda) \leq 0 \quad \text{for all } \lambda \in [\lambda_{\text{infl}}, \lambda_{\max}]$$

Finally,

$$\kappa'(\lambda_{\min}) \leq 0 \quad \text{and} \quad \kappa''(\lambda) \leq 0 \quad \text{for all } \lambda \in [\lambda_{\min}, \lambda_{\text{infl}}]$$

imply that

$$\kappa'(\lambda) \leq 0 \quad \text{for all } \lambda \in [\lambda_{\min}, \lambda_{\text{infl}}]$$

Therefore, **PC2** can be replaced by

$$n'(\lambda_{\max}) \leq 0 \qquad \kappa'(\lambda_{\max}) \leq 0 \qquad \kappa'(\lambda_{\min}) \leq 0$$

Summing up, the assumptions **PC1**–**PC4** will be satisfied if, and only if,

$$n(\lambda_{\max}) \geq 1 \qquad \kappa(\lambda_{\max}) \geq 0 \tag{55}$$

$$n'(\lambda_{\max}) \leq 0 \qquad \kappa'(\lambda_{\max}) \leq 0 \tag{56}$$

$$n''(\lambda) \geq 0 \quad \text{for all } \lambda \in [\lambda_{\min}, \lambda_{\max}] \tag{57}$$

$$\kappa''(\lambda) \geq 0 \quad \text{for all } \lambda \in [\lambda_{\text{infl}}, \lambda_{\max}] \tag{58}$$

$$\kappa''(\lambda) \leq 0 \quad \text{for all } \lambda \in [\lambda_{\min}, \lambda_{\text{infl}}] \tag{59}$$

$$\kappa'(\lambda_{\min}) \leq 0 \tag{60}$$

So, the continuous least-squares solution of the estimation problem is the solution $(d, n(\lambda), \kappa(\lambda))$ of

$$\boxed{\text{Minimize} \quad \int_{\lambda_{\min}}^{\lambda_{\max}} \left|T^{\text{calc}}\big(\lambda, s(\lambda), d, n(\lambda), \kappa(\lambda)\big) - T^{\text{meas}}(\lambda)\right|^2 d\lambda} \tag{61}$$

subject to the constraints (55)–(60).

For a given value of the thickness d, the constraints **PC1**, **PC2**, **PC3**, and **PC4** define a polyhedron P with nonempty interior in $\mathbb{R}^{2N}$. (The discretization of any pair of nonnegative, strictly convex, and decreasing functions n and α is an interior point of $\mathbb{P}$.) Therefore, the intersection of $\mathbb{P}$ with the set of points that satisfy (50) is nonempty, and defines a set of $\mathbb{R}^{2N}$ that, in general, contains more than one point. In principle, a global solution of (51), (55)–(60) could not be a unique solution of the estimation problem (which clearly exists in actual real-world situations because of physical reasons and, in numerical *gedanken* experiments, by construction). However, if the intersection of $\mathbb{P}$ with the set defined by (50) is small, we can expect that any (approximate) solution of (51), (55)–(60) is the closest to the true solution of the estimation problem. Theoretical verification of this fact is very hard, or even impossible, except for very small values of N, but an experimental study was designed in order to establish the reliability of the pointwise constrained optimization approach.

To illustrate the application of the above procedure, consider the optical transmission data of computer-generated films of known optical properties and thickness deposited onto a transparent substrate of known index of refraction. These *gedanken* experiments intend to simulate representative films for electronic applications. The goodness of the retrieval process is evaluated by comparing the retrieved values with the known solution. The transmission data, generated in the 500- to 1000-nm wavelength range, are rounded off to three digits to mimic the precision of the information normally available with experimental data. The simulation includes a glass substrate, assumed to be transparent in the spectral range under consideration. The numerical examples consider an absorption coefficient of the film having an exponential dependence on photon energy. The idea behind this particular choice of a rather steep $\alpha(\hbar\omega)$ is to investigate the powerfulness of the method for the retrieval of very small and very large α's.

The calculated transmittance of two films (1 and 2) of thickness 100 nm and 600 nm, respectively, is shown in Figure 15. As expected, film 1 does not show any fringe pattern in the

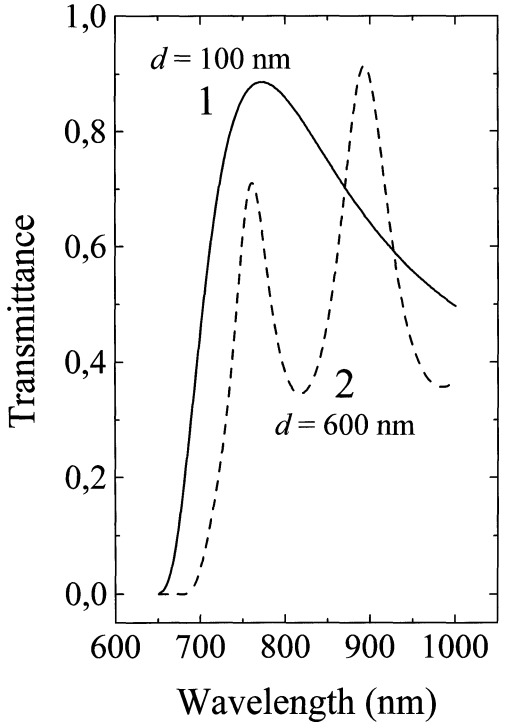

Fig. 15. Transmittance in the 650- to 1000-nm wavelength range of two computer-generated thin films supported by a transparent substrate of known properties. The thickness of the films 1 and 2 are 100 and 600 nm, respectively. Reproduced with permission from [36], copyright 1997, Optical Society of America.

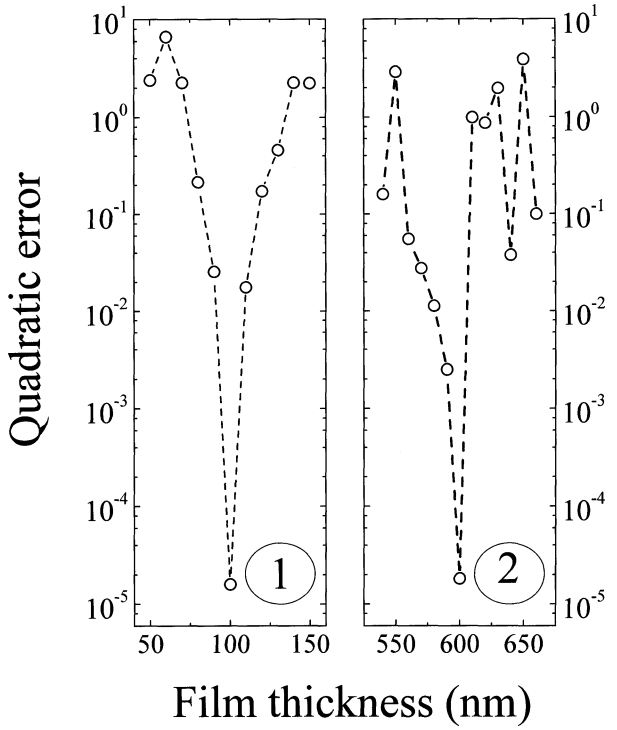

Fig. 16. Quadratic error of the minimization process as a function of trial thickness for films 1 and 2 of Figure 13. Note the excellent retrieval of the true thickness and the presence of local nonglobal minimizers. Reproduced with permission from [37], copyright 1998, Elsevier Science.

spectral range under consideration. Due to the photon energy dependence of the adopted α, and the film thickness, no transmission is measured for $\lambda < 650$ nm. Note that, using only the transmission data in the $650 \leq \lambda \leq 1000$ nm range, none of the films under consideration can be solved by approximate, or envelope, methods.

The results of the minimization process **as a function of the film thickness** d, which is the optimization variable, are shown in Figure 16. The least value of the quadratic error corresponds to the true film thickness. In the tests, the initial guesses for n and α are far from the values used to generate the transmission data. Figure 17 shows the retrieved optical constants of these *gedanken* films as a function of photon energy as given by the minimization process at the optimum thickness. They are compared in Figure 17 with the "true" values used to generate the transmission data. The precision of the retrieval is outstanding.

2.2.3. Unconstrained Optimization

The idea in the second approach [40] is to eliminate, as far as possible, the constraints of the problem, by means of suitable changes of variables. Roughly speaking, we are going to put the objective function of (61) as depending on the second derivatives of $n(\lambda)$ and $\kappa(\lambda)$ plus functional values and first derivatives at $\lambda_{\max}$. Moreover, positivity will be guaranteed expressing the variables as squares of auxiliary unknowns. In fact,

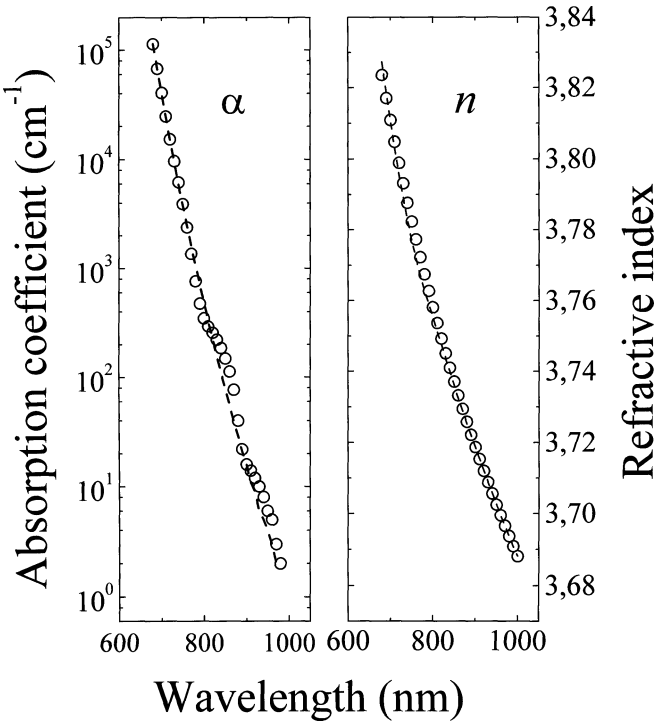

Fig. 17. Retrieved absorption coefficient and index of refraction of film 2 of Figure 13. Dashed line: α and n values used to calculate the transmittance shown in Figure 13. Open circles: retrieved α and n values. The agreement between original and retrieved values is very good.

we write

$$n(\lambda_{\max}) = 1 + u^2 \qquad \kappa(\lambda_{\max}) = v^2 \tag{62}$$

$$n'(\lambda_{\max}) = -u_1^2 \qquad \kappa'(\lambda_{\max}) = -v_1^2 \tag{63}$$

$$n''(\lambda) = \omega(\lambda)^2 \quad \text{for all } \lambda \in [\lambda_{\min}, \lambda_{\max}] \tag{64}$$

$$\kappa''(\lambda) = z(\lambda)^2 \quad \text{for all } \lambda \in [\lambda_{\text{infl}}, \lambda_{\max}] \tag{65}$$

$$\kappa''(\lambda) = -z(\lambda)^2 \quad \text{for all } \lambda \in [\lambda_{\min}, \lambda_{\text{infl}}] \tag{66}$$

At this point, in order to avoid a rather pedantic continuous formulation of the problem, we consider the real-life situation, in which data are given for a set of N equally spaced points on the interval $[\lambda_{\min}, \lambda_{\max}]$. So, we define

$$h = \frac{\lambda_{\max} - \lambda_{\min}}{N - 1}$$

and

$$\lambda_i = \lambda_{\min} + (i - 1)h \quad i = 1, \ldots, N$$

Consequently, the measured value of the transmission at λ_i will be called T_i^{meas}. Moreover, we will use the notation n_i, κ_i, ω_i, z_i in the obvious way:

$$n_i = n(\lambda_i) \qquad \kappa_i = \kappa(\lambda_i)$$

$$\omega_i = \omega(\lambda_{i+1}) \qquad z_i = z(\lambda_{i+1})$$

for all $i = 1, \ldots, N$. Discretization of the differential relations (62)–(66) gives

$$n_N = 1 + u^2 \qquad v_N = v^2 \tag{67}$$

$$n_{N-1} = n_N + u_1^2 h \qquad \kappa_{N-1} = \kappa_N + v_1^2 h \tag{68}$$

$$n_i = \omega_i^2 h^2 + 2n_{i+1} - n_{i+2} \qquad i = 1, \ldots, N-2 \tag{69}$$

$$\kappa_i = z_i^2 h^2 + 2\kappa_{i+1} - \kappa_{i+2} \quad \text{if } \lambda_{i+1} \geq \lambda_{\text{infl}} \tag{70}$$

$$\kappa_i = -z_i^2 h^2 + 2\kappa_{i+1} - \kappa_{i+2} \quad \text{if } \lambda_{i+1} < \lambda_{\text{infl}} \tag{71}$$

Finally, the objective function of (61) is approximated by a sum of squares, giving the optimization problem

$$\text{Minimize} \quad \sum_{i=1}^{N} \left[T^{\text{calc}}(\lambda_i, s(\lambda_i), d, n_i, \kappa_i) - T_i^{\text{meas}}\right]^2 \tag{72}$$

subject to

$$\kappa_1 \geq \kappa_2 \tag{73}$$

Since n_i and κ_i depend on $u, u_1, v, v_1, \omega, z$, and λ_{infl} through (67)–(71), the problem (72) takes the form

$$\boxed{\text{Minimize } f(d, \lambda_{\text{infl}}, u, u_1, v, v_1, \omega_1, \ldots, \omega_{N-2}, z_1, \ldots, z_{N-2})} \tag{74}$$

subject to (73). We expect that the constraint (73) will be inactive at a solution of (74), so we consider the unconstrained problem (74).

The unknowns that appear in (74) have different natures. The thickness d is a dimensional variable (measured in nanometers in our real-life problems) that can be determined using the data $T^{\text{meas}}(\lambda_i)$ for (say) $\lambda_i \geq \lambda_{\text{bound}}$, where λ_{bound}, an upper bound for λ_{infl}, reflects our prior knowledge of the physical problem. For this reason, our first step in the estimation procedure will be to estimate d using data that correspond to $\lambda_i \geq \lambda_{\text{bound}}$. To accomplish this objective, we solve the problem

$$\text{Minimize} \quad \overline{f}(u, u_1, v, v_1, \omega, z) \equiv \sum_{\lambda_i \geq \lambda_{\text{bound}}} \left[T^{\text{calc}}(\lambda_i, s(\lambda_i), d, n_i, \kappa_i) - T_i^{\text{meas}}\right]^2 \tag{75}$$

for different values of d, and we take as estimated thickness the one that gives the lowest functional value. In this case, the constraint (73) is irrelevant since it is automatically satisfied by the convexity of κ and the fact that the derivative of κ at $\lambda_{\min}$ is nonpositive. From now on, we consider that d is fixed, coming from the above procedure.

The second step consists of determining λ_{infl}, together with the unknowns u, u_1, v, v_1, ω, z. For this purpose, note that, given d and λ_{infl}, the problem

$$\text{Minimize} \quad \sum_{i=1}^{N} \left[T^{\text{calc}}(\lambda_i, s(\lambda_i), d, n_i, \kappa_i) - T_i^{\text{meas}}\right]^2 \tag{76}$$

is (neglecting (73)) an unconstrained minimization problem whose variables are u, u_1, v, v_1, ω, z ($2N$ variables). We solve this problem for several trial values of λ_{infl}, and we take as estimates of n and κ the combination of variables giving the lowest value. To minimize this function and to solve (75) for different trial thicknesses, we use the unconstrained minimization solver introduced in [41]. Let us emphasize at this point that the unconstrained optimization method has proven to be as reliable as the pointwise method. The comparison has been performed on numerically generated films and on real films deposited onto glass and onto crystalline substrates. We illustrate the point in the following subsection.

Testing the Algorithm with a-Si:H Films Deposited onto Glass Substrates. The unconstrained formulation applied to real thin films is considered now [43]. A series of a-Si:H samples with thicknesses varying from 100 nm to 1.2 μm, were deposited by the plasma decomposition of SiH_4 in a chemical vapor deposition (CVD) system under identical nominal conditions at an excitation frequency of 13.56 MHz. The deposition time was varied in order to produce films of different thickness but, otherwise, with identical properties. Figure 18 shows the optical transmission spectra of some samples of the series. The deposition time diminishes from (a) to (c), resulting in thinner films, as confirmed by a decreasing number of interference fringes. Note that the spectrum of sample 18a displays a reasonable fringe pattern in the region of weak absorption ($\lambda > 1000$ nm). The approximate properties of this film can be extracted from the position and the magnitude of the transmission maxima and minima appearing as an interference pattern [35]. However, the transmittance spectra of samples 18b and 18c, which possess a reduced (or absent) fringe pattern, can not be analyzed with envelope methods.

As already stated, the optimization process looks for a thickness that, subject to the physical constraints of the problem,

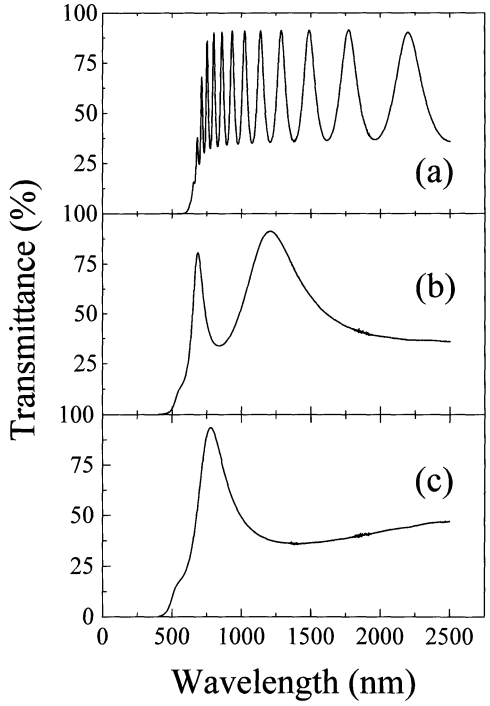

Fig. 18. Transmittance (%) versus wavelength of three a-Si:H films deposited onto glass of thickness: (a) 1220 nm, (b) 160 nm, and (c) 100 nm. Reproduced with permission from [43], copyright 2000, American Institute of Physics.

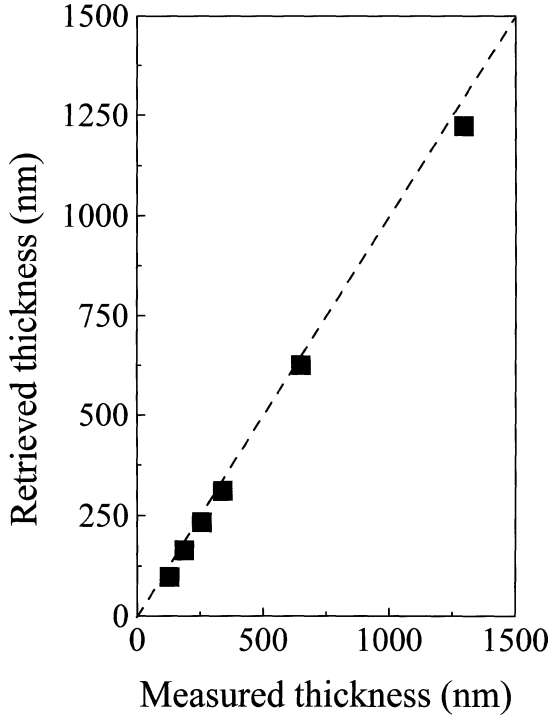

Fig. 19. Optically retrieved thickness versus mechanical measurement of a series of a-Si:H thin films. Reproduced with permission from [43], copyright 2000, American Institute of Physics.

minimizes the difference between the measured and the calculated spectra. The minimization starts sweeping a thickness range Δd_r divided into thickness steps Δd_s and proceeds decreasing Δd_r and Δd_s until the optimized thickness d_{opt} is found. In the present case, the starting Δd_r and Δd_s are 5 μm and 100 nm, respectively.

The thickness of the films can be measured by independent methods and compared with the ones obtained from the minimization process. To this aim, part of the deposited films was etched away and the height of the step (film thickness) measured with a Dektak profilometer. Figure 19 shows that the agreement between retrieved and measured thickness is very good for the whole series of samples. The small differences between optically and mechanically determined thickness may have several origins: (i) the precision and accuracy of the transmitted data may not be sufficient for a perfect thickness retrieval; (ii) there may be a relative error of the mechanical measurement; and (iii) there may exist a real thickness difference between the etched region and the region used for the transmittance measurements.

Figure 20 shows the retrieved optical constants of the films. The top part of Figure 20 displays the index of refraction n as a function of photon energy, different symbols being used for each film. Note that, for energies $\hbar\omega < 2.2$ eV, the indexes of refraction of all samples agree to a good extent. Although the films have been deposited under (nominally) identical conditions, and large differences in their properties are not expected, it is well known that the optical constants of a-Si:H films depend, to a certain extent, on film thickness. In that sense, we do

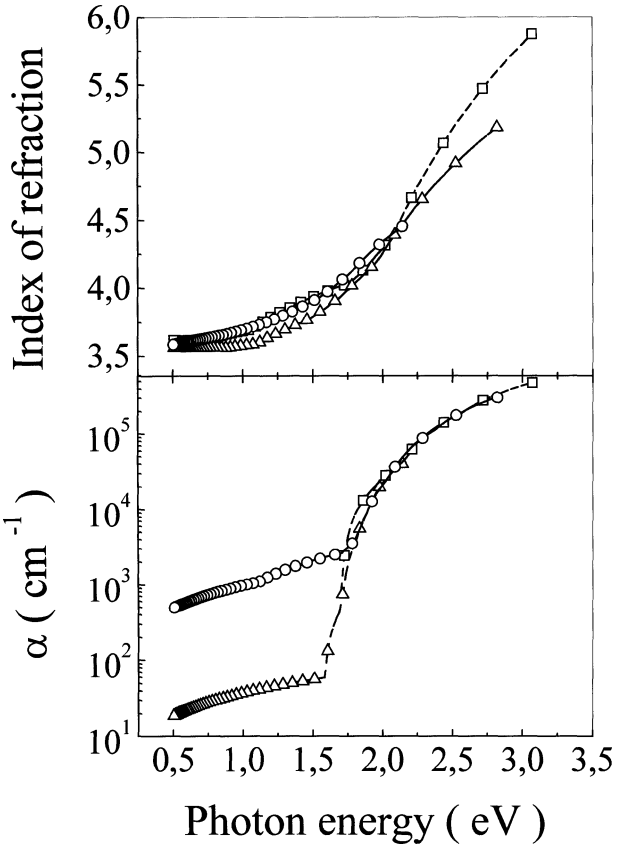

Fig. 20. Retrieved index of refraction and absorption coefficient of the films of Figure 16. Open circles: $d = 100$ nm; open squares: $d = 160$ nm; open triangles: $d = 1220$ nm. See text. Reproduced with permission from [43], copyright 2000, American Institute of Physics.

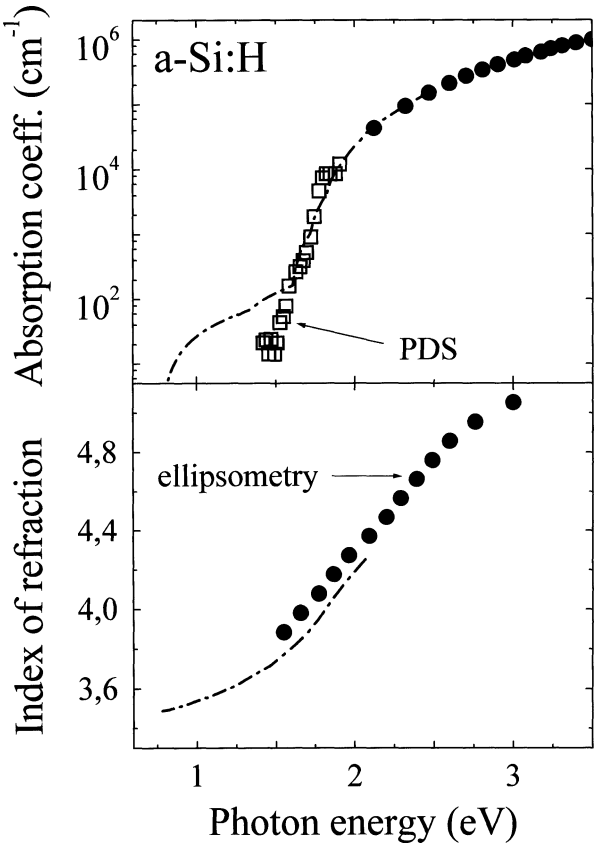

Fig. 21. Optical constants (dotted-dashed lines) retrieved from the transmittance data only of a 625-nm-thick a-Si:H film using the unconstrained optimization method. The retrieved values are compared with values measured on the same film with independent methods of characterization: ellipsometry and photothermal deflection spectroscopy. Reproduced with permission from [36], copyright 1997, Optical Society of America.

not expect that films having a thickness difference of more than one order of magnitude do display identical optical constants. The results shown in Figure 20, however, are a clear indication that the method works satisfactorily.

The bottom of Figure 20 shows the retrieved absorption coefficient α as a function of photon energy. The absorption coefficient at photon energies $\hbar\omega > 1.7$ eV is perfectly retrieved in all cases, even for the $d = 98$-nm-thick film. The retrieval of α at $\hbar\omega < 1.7$ eV depends, as expected, on film thickness. For a typical $d \approx 600$ nm a-Si:H film, values of α are correctly retrieved down to 100 cm^{-1}. The correctness of the retrieved optical constants has been confirmed in some samples by independent measuring techniques, that is, photothermal deflection spectroscopy and ellipsometry, as shown in Figure 21. Note that the absorption coefficient for the 625-nm-thick a-Si:H film shown in Figure 21 has been retrieved in a three-orders-of-magnitude span and down to 100 cm^{-1}. The small differences appearing between the retrieved refractive index and the ellipsometric determination of n may originate from the fact that, although the films have been grown simultaneously in the same run, they are deposited onto different substrates, glass for the optically retrieved n and crystalline silicon for the ellipsometric measurements. It is known that the nature of the substrate affects the properties of the films [36].

Summarizing, the unconstrained optimization method has been successful in retrieving the optical constants and the thickness of thin a-Si:H films (100 nm $< d <$ 1.2 μm) from transmittance data only. The method, being applicable to absorbing films and to films not displaying any fringe pattern, constitutes a significant improvement over other retrieval methods.

3. CONCLUSIONS

The simulation and optimization of the behavior of dielectric layered devices can be improved by means of the massive incorporation of well-known and novel techniques of numerical mathematics. We have given some examples throughout this work, but many open problems remain and many working programs can be traced taking into account the real needs of the industry. The following topics are the subject of current research in our group at the University of Campinas.

1. Although the solution of the basic direct problem is well known, the optimization of the calculations that lead to computing electric and magnetic fields in a multilayer structure is far from being complete. Fast calculations are important if we want to obtain practical and useful responses in reasonable time. The organization of computations in an optimal (or nearly optimal) way without loss of numerical stability is a problem area of most practical importance.

2. Related to the previous topic is the problem of computing the derivatives of the parameters to be estimated (for example, the thicknesses) in an optimal way. Techniques of automatic (or computational) differentiation are presently well known. However, in the presence of particular classes of problems, calculations can be much improved taking into account the specific characteristics of them. Roughly speaking, automatic differentiation involves two essential techniques: direct differentiation and reverse differentiation. The first is "easier," uses less memory, but is more time-consuming than the second. We are using direct differentiation in our present codes but we feel that combining this with the reverse mode and, especially, introducing the special features of the problems in a clever way, will improve both accuracy and efficiency of this computation. Needless to say, fast and accurate computation of derivatives is an essential ingredient for the efficacy of optimization algorithms.

3. We have worked in the reverse engineering problem related to the estimation of parameters of thin films for wavelengths in the infrared zone. We used very strongly empirical knowledge about the behavior of the refraction index and absorption coefficient for those wavelengths. Analogous techniques can be used for the estimation of other types of materials using data in different spectral zones, if we employ in a suitable way phenomenological and empirical knowledge of the parameters to be estimated on those zones.

4. Current models for thin-film estimation are based on transparent substrates. This is an oversimplification since, in na-

ture, such types of materials do not exist and the ones available in commerce (glasses, sapphire, c-Si, etc.) have nonnegligible absorption coefficients. Moreover, both models and practical experiments show that the substrate thickness (associated, of course, to its absorption) has a meaningful effect on the transmission measures. It seems, thus, that more comprehensive models that take into account the substrate thickness and its absorption could represent more accurately the reality and, in the estimation problem, could provide better guesses of the optical parameters.

5. More complex models for transmission and reflection can involve averaging of the responses over ranges of wavelengths (or thicknesses, or incidence angles, or polarization angles). The oscillatory behavior of light causes large variations of the functions to be integrated over small ranges of the integration parameter. Therefore, numerical integration procedures are very expensive (they demand thousands of integration points) and analytical methods are generally impossible. The practical consequence is that optimization procedures based on merit functions that involve those models could be very slow. On one hand, this means that the development of fast and accurate problem-oriented quadrature methods is necessary. On the other hand, optimization algorithms oriented to "expensive functions" must be used, and many methods exploiting the special features of our problems are yet to be discovered.

7. All the inverse problems considered in this work are "global optimization problems" in the sense that we are interested in the absolute minimizer of the merit functions and not, merely, in a local minimizer. However, these problems are not convex and, generally, possess many local minimizers and stationary points. Algorithms for global minimization have been devised in the last 30 years, since this is, probably, the most important problem in the broad area of optimization. However, no algorithm can guarantee to find global minima in reasonable time for a reasonably large scope of functions. Moreover, there is not a sufficiently comprehensive theory that explains the behavior of global optimization methods and serves as a guide for the invention of new ones. It is not surprising, thus, that we generally use "local" optimization methods for solving global optimization problems, with the hope that they will work, perhaps with the help of judicious or repetitive choices of initial points. It is worth mentioning that some successful optimization algorithms consist of strategies for changing initial points, after finding probable local minimizers using local optimization. In any case, when one is in the presence of a practical problem, useful global optimization procedures are the ones that exploit the problem characteristics. To a large extent, this has yet to be done in many of our estimation problems. There is still a paradox in the consideration of this item. In inverse problems, it is not always true that the global optimizer of the "obvious" merit function is the best estimate. If the problem is very ill-conditioned and the data are subject to errors, the "true solution" can have no meaning at all. The art of finding a good merit function (by means of, perhaps, regularization techniques) is an independent problem that has been exhaustively studied in many particular engineering problems.

8. In filter design problems, we require a certain behavior of the reflectance or the transmittance over a relative large range of wavelengths. Usually, we deal with that requirement by means of an ad hoc objective (merit) function. For example, if we want small reflectance over the range $[\lambda_{\min}, \lambda_{\max}]$, we minimize the sum of reflectance over that range. However, this approximation does not reflect exactly our requirement: a reflectance smaller than (say) 0.1% can be perfectly satisfactory, and it is not worthwhile to waste "optimization effort" in improving it if such a goal has been attained. A more adequate model could be to express the requirements as a set of inequalities such as (say) "Reflectance $<0.1\%$ for "all" λ in $[\lambda_{\min}, \lambda_{\max}]$." In this case, the design procedure does not require unconstrained or simple-constrained optimization as before, but rather nonlinearly constrained optimization (with many constraints!). Moreover, the constraints are not absolutely independent since, obviously, the response at some wavelengths is related to the response at their neighbors. Finally, the variations of the response with respect to the wavelength make it uncertain how many (and which) wavelengths must be involved in the optimization. All these considerations lead to more complex models than the ones considered up to now, at least, under the optimization framework. They represent in a closer way the practical requirements of calculations, but it is not clear whether their practical implementation is invalidated by their complexity, with the present state of computational architectures.

10. Practical designs of filters usually include "sensitivity requirements." We wish not only a given response for given wavelengths but also some stability with respect to thickness variations, since it is not realistic to assume that films with arbitrary mathematical thickness precision could be synthesized. It is relatively easy to analyze the sensitivity of a given solution, but the challenging question is to incorporate the sensitivity requirement in the original problem, in a correct mathematical-modelling framework and in a realistic way from the practical point of view.

11. A broad interface field between numerical mathematics and the engineering electronic devising field that deserves a great deal of further exploiting is "solar-cell optimization." The direct-problem mathematics related to modelling the incidence of solar rays on this type of devices seems to be sufficiently understood, but there are many optimization problems that need to be solved in practice. Solar rays do not fall vertically and with uniform intensity during all day, all year, and in different regions of the world. Incorporating these real features into models aiming to optimize materials, dimensions, and angles could be of maximal practical and economical significance.

Acknowledgment

This work was partially supported by the Brazilian agencies: Fundação de Amparo à Pesquisa do Estado de São Paulo (FAPESP) and Conselho Nacional de Desenvolvimento Científico e Tecnológico (CNPq).

REFERENCES

1. I. Newton, in "Optics." Great Books, Vol. 34. Encyclopedia Britannica, Chicago, 1952.
2. C. Huygens, in "Treatise on Light." Great Books, Vol. 34. Encyclopedia Britannica, Chicago, 1952.
3. L. Euler, in "Lettres a une Princesse d'Allemagne," pp. 86–100. Courcier Editeurs, Paris, 1812.
4. T. Young, "A Course of Lectures on Natural Philosophy and the Mechanical Arts." Johnson, London, 1807; Johnson, New York, 1971.
5. J. F. W. Herschel, "Natural Philosophy," p. 258. A. & R. Spottiswoode, London, 1831.
6. C. Coulston Gillespie, Ed., "A Diderot Pictorial Encyclopaedia of Trades and Industry," Plates 255 and 256. Dover Publications, New York, 1959.
7. A. N. Tikhonov and V. Ya. Arsenin, "Solution of Ill-Posed Problems." Winston-Wiley, New York, 1977.
8. M. Born and E. Wolf, "Principles of Optics," 6th ed. Pergamon Press, United Kingdom, 1993.
9. O. S. Heavens, "Optical Properties of Thin Solid Films." Dover Publications, New York, 1991.
10. R. A. Smith, "Semiconductors," 2nd ed. Cambridge University Press, London, 1979.
11. M. L. Cohen and J. Chelikowsky, "Electronic Structure and Optical Properties of Semiconductors," 2nd ed. Springer Series on Solid State Science, Vol. 75. Springer-Verlag, Berlin, Heidelberg, 1989.
12. P. T. Yu and M. Cardona, "Fundamentals of Semiconductors." Springer-Verlag, Berlin, Heidelberg, 1996.
13. S. H. Wemple and M. DiDomenico, Jr., *Phys. Rev. B* 3, 1338 (1971).
14. G. D. Cody, in "Semiconductors and Semimetals," Vol. 21, Part B, (J. Pankove, Ed.). Academic Press, New York, 1984.
15. A. R. Zanatta, M. Mulato, and I. Chambouleyron, *J. Appl. Phys.* 84, 5184 (1998).
16. F. Abeles, *Rev. Opt*. 32, 257 (1953); also *J. Opt. Soc. Am*. 47, 473 (1957).
17. H. M. Liddell, "Computer-Aided Techniques for the Design of Multilayer Filters." Adam Hilger, Bristol, UK, 1980.
18. H. A. Macleod, "Thin Film Optical Filters." Adam Hilger, Bristol, UK, 1969.
19. A. Friedlander, J. M. Martínez, and S. A. Santos, *Appl. Math. Optim.* 30, 235 (1994).
20. `www.ime.unicamp.br/~martinez`
21. A. V. Tikhonravov, M. K. Trubetskov, and G. W. DeBell, *Appl. Optics* 35, 5493 (1996).
22. See *Tech. Dig. Ser.-Opt. Soc. Am.* 9, 236 (1998).
23. A. Friedlander and J. M. Martínez, *SIAM J. Optim.* 4, 177 (1994).
24. R. H. Bielschowsky, A. Friedlander, F. M. Gomes, J. M. Martínez, and M. Raydan, *Investigación Operativa* 7, 67 (1998).
25. J. E. Dennis and R. B. Schnabel, "Numerical Methods for Unconstrained Optimization and Nonlinear Equations." Prentice-Hall, Englewood Cliffs, NJ, 1983.
26. O. S. Heavens, "Thin Film Physics." Methuen, London, 1970.
27. G. Hass, Ed., "Physics of Thin Films." Academic Press, New York, 1960.
28. Z. Knittl, "Optics of Thin Films." Wiley, Czechoslovakia, 1976.
29. L. Eckertova, "Physics of Thin Films," 2nd ed. Plenum, New York, 1986.
30. M. Ward, "The Optical Constants of Bulk Materials and Films." Institute of Physics, UK, 1994.
31. R. L. Mooney, *J. Opt. Soc. Am.* 35, 574 (1945).
32. Commission of the European Communities, Document EUR 6423 (1979).
33. A. M. Goodman, *Appl. Opt.* 17, 2779 (1978).
34. J. C. Manifacier, J. Gasiot, and J. P. Fillard, *J. Phys. E: Sci. Instrum.* 9, 1002 (1976).
35. R. Swanepoel, *J. Phys. E: Sci. Instrum.* 16, 1214 (1983); 17, 896 (1984).
36. I. Chambouleyron, J. M. Martinez, A. C. Moretti, and M. Mulato, *Appl. Opt.* 36, 8238 (1997).
37. I. Chambouleyron, J. M. Martinez, A. C. Moretti, and M. Mulato, *Thin Solid Films* 317, 133 (1998).
38. R. B. Murtagh and M. A. Saunders, MINOS User's Guide, Report SOL 77-9, Department of Operations Research, Stanford University, CA, 1977.
39. R. B. Murtagh and M. A. Saunders, *Math. Program.* 14, 41 (1978).
40. E. G. Birgin, I. Chambouleyron, and J. M. Martínez, *J. Comp. Phys.* 151, 862 (1999).
41. M. Raydan, *SIAM J. Optim.* 7, 26 (1997).
42. E. G. Birgin, Ph.D. Thesis, IMECC-UNICAMP, Brazil, 1998. [In Portuguese.]
43. M. Mulato, I. Chambouleyron, E. G. Birgin, and M. Martínez, *Appl. Phys. Lett.* 77, 2133 (2000).